American Mineralogist, Volume 71, pages 376–395, 1986

Magmatic-hydrothermal transition in the Tanco rare-element pegmatite: Evidence from fluid inclusions and phase-equilibrium experiments

DAVID LONDON
School of Geology and Geophysics, University of Oklahoma, Norman, Oklahoma 73019

ABSTRACT

Fluid inclusions in petalite, spodumene, eucryptite, and coexisting quartz from the Tanco mine, Manitoba, have been evaluated with respect to experimentally calibrated reaction relationships in the system $LiAlSiO_4$-SiO_2 to define the cooling path and fluid evolution within this pegmatite. At Tanco, the conversion of petalite to pseudomorphic intergrowths of spodumene + quartz occurred at approximately 500°C and 3000 bars in the presence of a dense hydrous alkali borosilicate fluid with a minor carbonate component. Between 470 and 420°C and between 2900 and 2600 bars, the borate component of this fluid was removed by the crystallization of tourmaline, resulting in the deposition of albite, micas, quartz, and ore minerals (e.g., microlite, beryl, and pollucite), and consequent evolution of a comparatively low-density, solute-poor, CO_2-bearing aqueous fluid (approximately 91 mol% H_2O, 5 mol% CO_2, 4 mol% NaCl equivalent). Reactions over this P-T interval mark the transition from magmatic to subsolidus hydrothermal conditions. Ore-bearing albitic (aplite or cleavelandite) units probably were deposited directly from the borosilicate fluid and are not the result of subsolidus metasomatism.

INTRODUCTION

Pioneering experimental studies of granitic systems by R. H. Jahns and his colleagues have provided a starting point for understanding the petrogenesis of pegmatites (e.g., Jahns and Burnham, 1958, 1969; Burnham and Jahns, 1961; Luth et al., 1964); however, comparatively little progress has been made in defining the formation conditions of lithium-rich, rare-element pegmatites in terms of changes in pressure, temperature, and compositions of pegmatitic fluids (e.g., Černý, 1982; Norton, 1983). With the experimental calibration of the lithium aluminosilicate phase diagram (London, 1984a), it is now possible to combine lithium aluminosilicate reaction relationships with fluid-inclusion data to define emplacement conditions, cooling histories, and fluid evolution in some lithium-rich pegmatites. This paper presents the results of one such study of the Tanco pegmatite, Manitoba, and its general implications for rare-element pegmatites and granites.

Most petrologists agree that an aqueous-fluid phase plays an important role in the generation of pegmatites. Present views regarding the compositions and physical properties of pegmatitic aqueous fluids are varied and largely conjectural. Observations drawn from experiments in compositionally simple systems (e.g., silica-H_2O, albite-H_2O, haplogranite-H_2O) have led some petrologists to propose that pegmatitic aqueous fluids possess relatively low solute concentrations (e.g., Stewart, 1978; Roedder, 1981, 1984; see Jahns, 1982, for a review of the relevant experimental literature). Rare-element pegmatites, however, contain minerals rich in Li, B, and F. Addition of these hyperfusible components (and possibly others such as Be, Rb, Cs, and P) to granitic systems alters partitioning coefficients for major and minor elements, lowers solidus and liquidus temperatures, and generally increases silicate liquid–H_2O miscibility (e.g., Wyllie and Tuttle, 1961, 1964; Koster van Groos and Wyllie, 1968; Kovalenko et al., 1973; Chorlton and Martin, 1978; Manning, 1981; Martin, 1983; Pichavant, 1981, 1983; Pichavant and Ramboz, 1985; Benard et al., 1985). Several studies of fluid inclusions in pegmatite minerals already have presented empirical evidence for the existence of dense aqueous fluids or brines that contain up to 85 wt% dissolved silicate and salt components (e.g., Lemmlein et al., 1962; Roedder, 1963; Kozlowski and Karwowski, 1973; Bazarov, 1975). Thus, aqueous fluids in rare-element pegmatites may have solute concentrations (especially with regard to aluminosilicate components) that are far greater than those generated in the simple silicate-H_2O experiments on which existing pegmatite models are based (e.g., see Norton, 1983).

One potentially valuable means of tracing the evolution of pegmatitic fluids is through examination of the fluid inclusions that are abundant in pegmatite minerals. Soviet petrologists have conducted numerous investigations of fluid inclusions in minerals from rare-element pegmatites (e.g., Lemmlein et al., 1962; Makagon, 1973; Orlova and Bazarov, 1975; Bazarov and Orlova, 1976; Kazamirova, 1976; Litovchenko, 1976; Boyarskaya et al., 1977; Rossovskii et al., 1978; Rossovskii, 1981). Most of the Soviet studies are difficult to evaluate, either because only abstracts of the work are available (in Roedder, 1968–1985)

0003–004X/86/0304–0376$02.00

or because the work suffers from incompleteness or from poor documentation of the properties of the inclusions studied. In contrast to the large number of studies conducted by Soviet petrologists, relatively few investigations of fluid inclusions in rare-element pegmatites have been performed by Western scientists (see Weiss, 1953; Cameron et al., 1953; Foord, 1976; Taylor et al., 1979; Cook, 1979; Brookins et al., 1979). As with the Soviet work, however, the most significant shortcoming is from the lack of a suitable independent *P-T* reference for evaluation of inclusion origin (primary vs. secondary) and entrapment conditions (cf. Weisbrod and Poty, 1975).

A study of lithium aluminosilicate stabilities has yielded an experimentally quantified *P-T* phase diagram that constitutes a petrogenetic grid for many lithium-rich pegmatites (London, 1981, 1984a; London and Burt, 1982b). At the largest-known rare-metal–producing pegmatites (e.g., Tanco, Manitoba; Harding, New Mexico; Bikita, Zimbabwe; Londonderry, Western Australia), two or all three of the lithium aluminosilicates occur together with quartz. In these important cases, data from fluid inclusions in petalite ($LiAlSi_4O_{10}$), spodumene (α-$LiAlSi_2O_6$), and eucryptite (α-$LiAlSiO_4$) and cogenetic quartz can be combined with reaction relationships among lithium aluminosilicates to establish well-constrained *P-T* paths and to characterize fluids at the middle to late stages of pegmatite consolidation during which rare-metal ores are deposited.

The Tanco mine at Bernic Lake, Manitoba, is developed in a large (1440 × 820 m), subhorizontal granitic pegmatite that is enriched in Li, Be, Rb, Cs, Sn, and Ta (Crouse et al., 1979). Lithium minerals occur principally as lithium aluminosilicates located in the central parts of the pegmatite. The occurrence of lithium aluminosilicates at Tanco is notable in that petalite, spodumene, and eucryptite occur together with quartz. Textural evidence indicates that primary petalite was extensively replaced by an isochemical intergrowth of spodumene + quartz, and that minor amounts of spodumene and relic petalite were subsequently altered to eucryptite + quartz (Černý and Ferguson, 1972; Černý, 1975). Therefore, crystallization of the Tanco pegmatite followed a *P-T* path that passed above but near the invariant point containing these three lithium aluminosilicates plus quartz in the system $LiAlSiO_4$-SiO_2 (London, 1981, 1984a; London and Burt, 1982b). The constraints on the *P-T* path as defined by the lithium aluminosilicate assemblages at Tanco provide the frame of reference by which fluid-inclusion data have been interpreted.

Table 1. Microthermometric data

PETALITE

aqueous

Te = -48(3)°C[10]
Tm ice = -3.1(2.2)°C[17]

mixed H_2O-CO_2

Tm calthrate = 4.7(1.1)°C[8]

SPODUMENE

Crystal-rich, in coarse laths and pseudomorphs after petalite

Te = -49(3)°C[65]
Tm ice = -4.6(2.0)°C[101] (all)
Th LV = 293(34)°C[292] (laths)
= 315(23)°C[216] (pseudomorphs)
Tm dms = 370(10)°C (solidus)
= 470(10)°C (liquidus)

Secondary aqueous, coarse laths only

Te = -68(10)°C[40]
Tm ice = -29.9(2.5)°C[66]
Th LV = 175(12)°C[60]

QUARTZ

Pseudomorphs After Petalite:

(1) mixed H_2O-CO_2

Tm clathrate = 4.1(2.8)°C [36]
Th LV = 289(14)°C [77]

(2) aqueous

Te = -69(6)°C [60]
Tm ice = -15.1(4.2)°C [113]
Th LV = 195(26)°C [275]

(3) pure-CO_2

Te = Tm CO_2 = -56.9(0.3)°C [58]
Th LV = 5.6(3.7)°C [264]

Massive Quartz

(1) mixed H_2O-CO_2

Te = -55.3(1.8)°C [7]
Tm clathrate = 5.2(0.9)°C [88]
Th LV = 282(7)°C [47]

(2) aqueous Group I

Te = -59(1)°C [6]
Tm ice = -7.2(1.9)°C [32]
Th LV = 213(10)°C [82]

(3) aqueous Group II

Te = -75(5)°C [61]
Tm ice = -20.2(4.3)°C [66]
Th LV = 184(8)°C [95]

(4) aqueous Group III

Te < -100°C
Tm ice = -57.5(0.5)°C [64]
Th LV = 139(15)°C [137]

Miarolytic Cavity

(1) mixed H_2O-CO_2

Te (ice) = -48(1)°C [25]
Tm clathrate = 6.0(0.9)°C [86]
Th LV = 285(8)°C [57]

(2) aqueous Group I

Te = -66(3)°C [48]
Tm ice = -12.2(2.2)°C [201]
Th LV = 205(17)°C [243]

(3) aqueous Groups II and III

Te = -73(1)°C [18] (Group II)
= -79(2)°C [24] (Group III)
Tm ice = -23.6(3.4)°C [35] (Group II)
= -37.0(2.0)°C [22] (Group III)
Th LV = 152(9)°C [137] (Groups II and III)

EUCRYPTITE + QUARTZ (BOTH MINERALS)

(1) aqueous

Te = -72(4)°C [41]
Tm ice = -25.6(8.6)°C [125]
Th LV = 142(25)°C [140]

(2) pure-CO_2

Te = Tm CO_2 = -56.5(0.2)°C [8]
Th LV = 22.4(2.2)°C [14]

Reported values are arithmetic mean, followed by standard deviation ( ), and number of observations [ ]

Analytical methods

Most microthermometric measurements were performed on a Linkam TH600 heating and freezing stage at the University of Oklahoma; the Linkam system was calibrated between −57°C and +307°C with respect to melting points of 25 standard or spectroscopic grade compounds. Additional microthermometry was conducted on a calibrated Linkam stage at the University of Toronto and a Chaix-Meca stage at the U.S. Geological Survey, Reston, Virginia. The heating-freezing stages were used to obtain temperatures of the first appearance of liquid upon heating a frozen inclusion (eutectics, T_e); final disappearance of ice (T_m ice), solid CO_2 (T_m CO_2), and CO_2 clathrate (T_m clathrate); liquid-vapor homogenization (T_h LV); dissolution or melting of daughter minerals (T_m dms); and inclusion decrepitation (T_d). The symbol T_h LV is used to denote homogenization of H_2O(l)-H_2O(v), CO_2(l)-CO_2(v), and H_2O(l)-CO_2(l); all inclusions homogenized to the denser (liquid) phase. Electron images and energy-dispersive analyses of included crystalline solids and quenched glasses were obtained on an ETEC Autoscan electron microscope (SEM) and Princeton Gamma-Tech System II energy-dispersive spectroscopic analyzer (EDS) at the University of Oklahoma, and a JEOL-35 SEM with Tracor-Northern 1700 EDS at the Geophysical Laboratory, Washington, D.C.

Properties of fluid inclusions

Microthermometric data are presented in Figures 1 and 5, and are summarized in Table 1. Equation 2 of Potter et al. (1978) was used to calculate salinities of aqueous fluids in inclusions that contained no CO_2; determination of aqueous-liquid salinity in mixed H_2O-CO_2 was performed by comparison of measured clathrate-disappearance temperature to Figure 2 of Collins (1979). Densities of homogeneous aqueous liquids in CO_2-absent inclusions

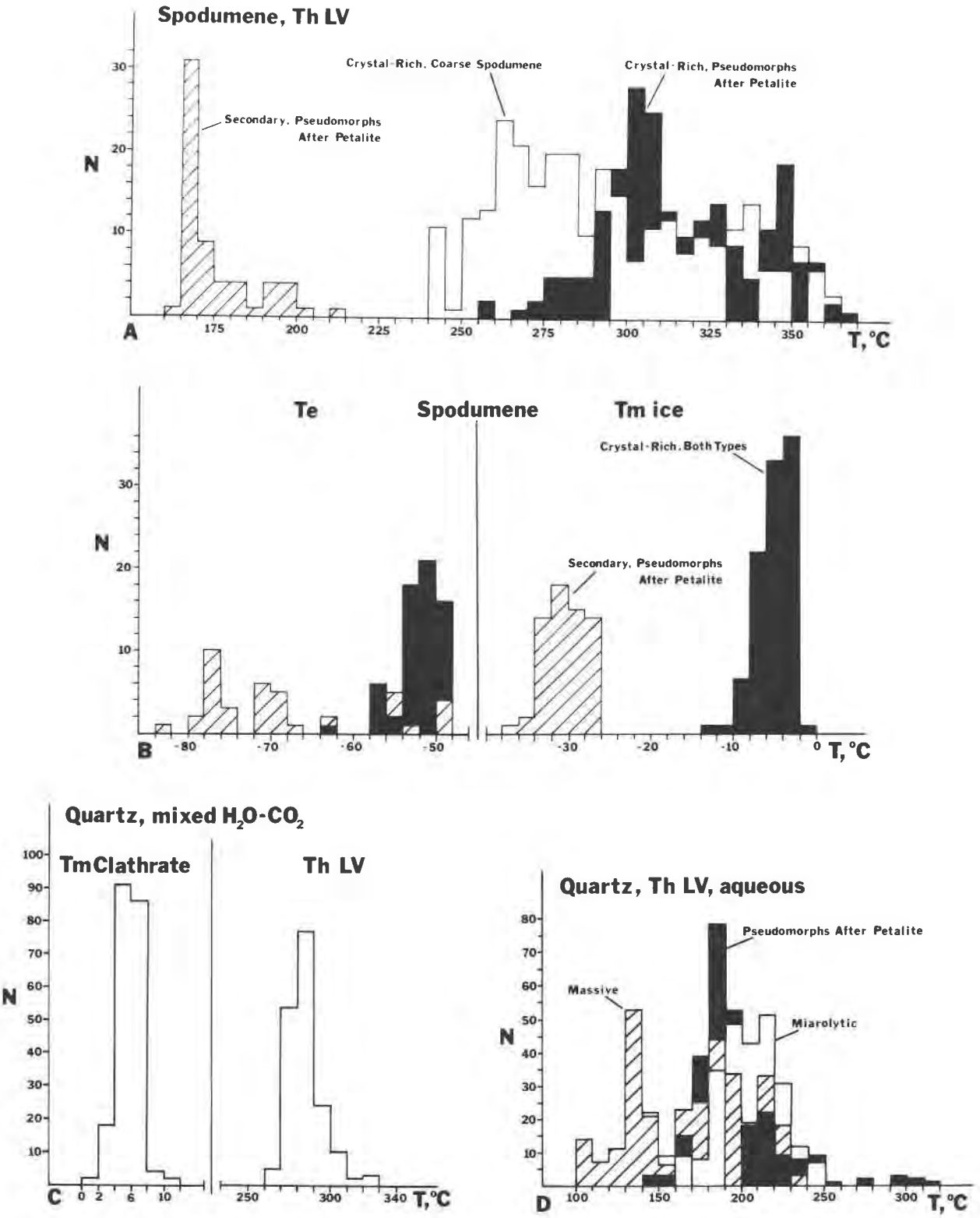

Fig. 1. Histograms of microthermometric data. Individiual bar graphs are superimposed, not stacked.

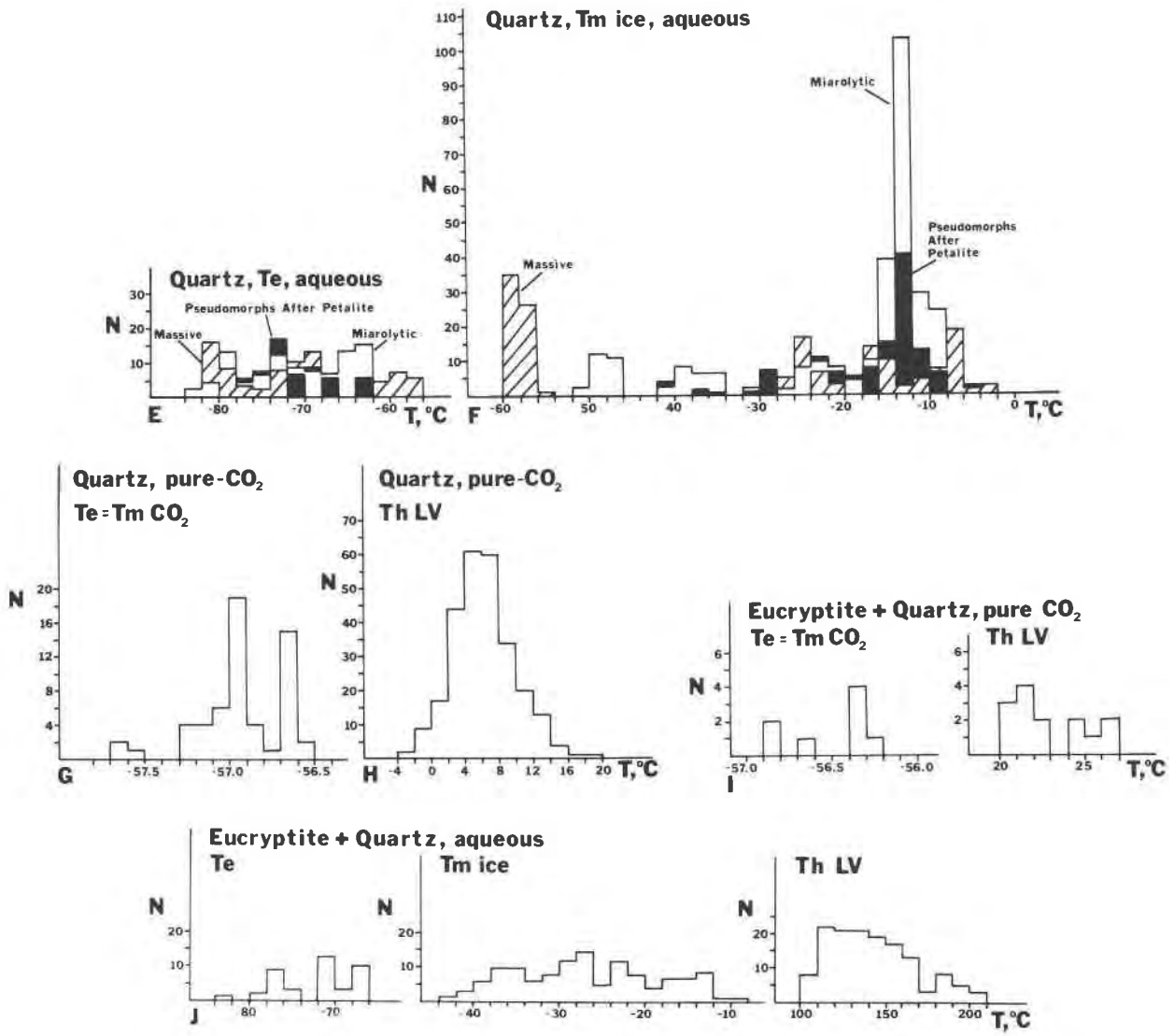

Fig. 1—*Continued.*

were calculated from Equation Al of Bodnar (1983); densities of pure-CO_2 fluids are determined from Angus et al. (1973); densities of mixed H_2O-CO_2-salt (assumed NaCl equivalence) fluids are taken from Bowers and Helgeson (1983b). Isochores are constructed by application of pertinent graphical data in Roedder and Bodnar (1980), Hollister (1981), and Bowers and Helgeson (1983b). Reported numerical values in the text and in Table 1 are given in the following sequence: arithmetic mean, one standard deviation in parentheses (), and number of measurements in brackets [].

Spodumene and petalite

Spodumene is abundant in several pegmatitic zones as relatively fine-grained laths (up to 10 cm) intergrown with quartz as pseudomorphs after petalite, and as coarse-grained crystals (up to 1.5 m) embedded in massive quartz, rarely with microcline or montebrasite (Černý and Ferguson, 1972; Černý, 1975). Both textural types of spodumene are densely packed with crystal-filled fluid inclusions (approaching 1.0 vol% of the host phase) that are similar in morphology and content throughout all samples from widely separated portions of the pegmatite.

Most inclusions are large (average 50 × 20 × 10 μm, but up to 2 mm in length), possess subhedral to euhedral negative crystal forms of the host spodumene, and are distributed in dense three-dimensional clusters, as isolated individuals, and as planar clusters on {110} and along fractures (Figs. 2B–2D).

At 25°C, most inclusions contain a relatively low salinity aqueous liquid (7.3(3.0) equivalent wt% NaCl) and H_2O vapor (Table 1 and Fig. 1). Traces of K, Ca, Mg, Cl, and S were occasionally detected by EDS as thin efflorescent films on the walls of opened inclusions. The low eutectics

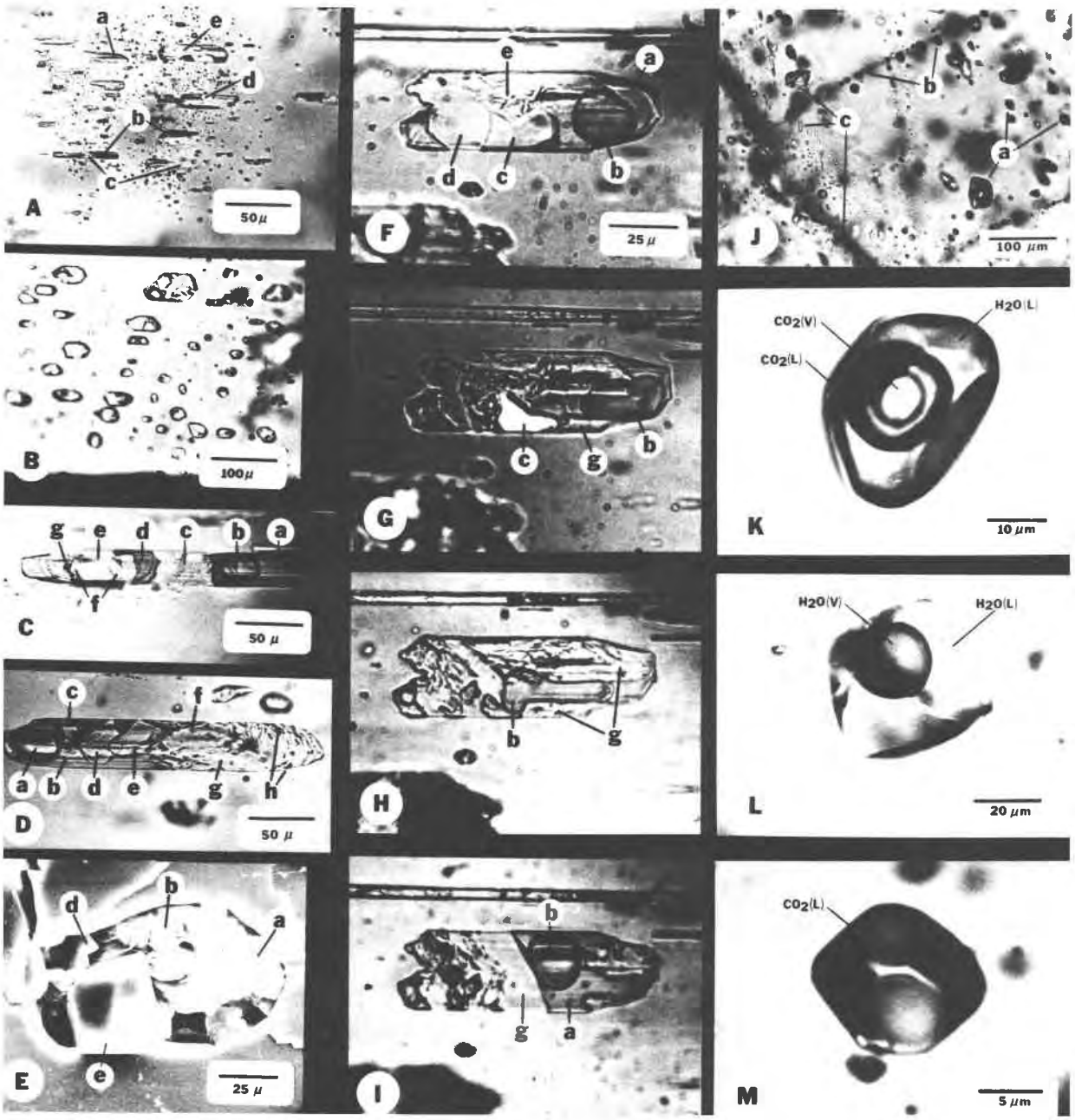

Fig. 2. Fluid inclusions in petalite, spodumene, and quartz.

A. Fluid inclusions in petalite. Contents at 25°C (partially crossed polars) appear to be (a) H_2O-rich liquid, (b) H_2O vapor, (c) cookeite, (d) lithium tetraborate, and (e) albite.

B. Doubly polished chip of spodumene after petalite (partially crossed polars at 25°C).

C. A crystal-rich inclusion in coarse-grained spodumene (partially crossed polars at 25°C). The inclusion contains (a) H_2O-rich liquid, (b) H_2O vapor, (c) cookeite, (d) lithium tetraborate, $Li_2B_4O_7$, (e) albite, (f) unidentified daughter minerals that (in EDS analyses of opened inclusions) are either quartz or pollucite-analcime solid solution, and (g) microlite (?) (reprinted from London, 1985).

D. Crystal-rich inclusion in coarse-grained spodumene near the tip of a large crystal. Contents (at 25°C, partially crossed polars) are (a) H_2O vapor, (b) H_2O-rich liquid, (c) rhombohedral (lithium or beryllium) carbonate, (d) $Li_2B_4O_7$, (e) albite or pollucite, (f) albite, (g) cookeite, (h) brown isotropic phase that appears to be microlite.

E. An SEM image of a crystal-rich inclusion in spodumene; contents are (a) albite, (b) cookeite, (c) quartz, (d) $Li_2B_4O_7$ (reprinted from London et al., 1982).

F–I. Homogenization of crystal-rich inclusions in spodumene under external hydrothermal pressure to prevent decrepitation (reprinted from London et al., 1982). Before runs (F, plane-polarized light at 25°C), this inclusion contained (a) H_2O-rich liquid, (b) H_2O vapor, (c) cookeite, (d) lithium tetraborate, and (e) albite. After quench from 375°C (G, partially crossed polars), the daughter

(Table 1 and Fig. 1) could reflect a complex salt solution, perhaps dominated by divalent metal cations (see Crawford, 1981); however, the microthermometric properties also may be modeled after a solution of $Li_2B_4O_7$ (T_e = −15 (2)°C [10], T_m ice = −1.6(0.1)°C [8]; n.b. that details of the phase equilibria of $Li_2B_4O_7$-H_2O solutions are complex and not yet fully resolved), which has been identified in spodumene-hosted inclusions from Tanco.

Virtually all inclusions are crystal-rich, although variations from crystal-rich to crystal-absent inclusions do exist (the significance of variable crystal/liquid proportions is discussed in Interpretation of Inclusion Data). The included solids appear to constitute an equilibrium mineral assemblage that is remarkably consistent throughout all samples (Fig. 2B); thus, these phases are regarded as daughter minerals (as opposed to accidentally trapped solids). On the basis of optical examination, EDS analyses of 87 grains within opened inclusions (e.g., Fig. 2E), and Gandolfi camera X-ray diffraction patterns, the daughter minerals have been identified as albite, cookeite ($LiAl_5Si_3O_{10}(OH)_8$), pollucite-analcime solid solution ($CsAlSi_2O_6 \cdot H_2O$-$NaAlSi_2O_6 \cdot H_2O$), quartz, and lithium tetraborate, $Li_2B_4O_7$ (the new mineral species diomignite: D. London, M. E. Zolensky, E. Steele, and E. Roedder, unpub. data, 1985). In addition to $Li_2B_4O_7$, inclusions near the tips of coarse-grained spodumene laths also contain a carbonate that breaks down to yield CO_2 fluid at $T >$ 400°C (see discussion of crystal homogenization runs below). Although calcite has been reported from the spodumene-rich zones (Černý, 1972a), none has been found in EDS analyses of daughter minerals.

Aqueous fluids in crystal-rich inclusions homogenize over the range 240 to 350°C. Inclusions in the fine-grained spodumene pseudomorphs after petalite homogenize between 255 and 370°C with a mean of 315(23)°C [216] (Table 1 and Fig. 1). Inclusions in the cores of large, primary laths display a similar range of homogenization temperatures with a slightly lower mean value and continuously decreasing homogenization temperatures outward toward the tips of crystals. The range of T_h LV for most inclusion clusters was less than 20°C; T_h LV for groups of inclusions that showed conspicuous evidence of necking down (mostly along healed fractures and {110}) are not included in the homogenization data of Table 1 and Figure 1.

Daughter minerals generally show little sign of melting or dissolution into the aqueous fluid up to T_d = 325–375°C (except as discussed below). Reactions among daughter minerals were monitored by sealing chips of spodumene in Pt-foil capsules for runs in conventional cold-seal hydrothermal reaction vessels at external P_{H_2O} = 2 kbar (pressure on the spodumene host to prevent decrepitation) and T = 325–550°C for 5–24 h. Runs were quenched with an air/water jet to $T <$ 300°C in approximately 10 s. Thirty such runs at 25°C intervals revealed that solid phases in approximately 95% of the inclusions melt to a quenchable glass or gel (plus aqueous liquid that exsolved on quench) between 370°C (start of solution) and 470°C (liquidus or complete crystal-solution homogenization) (Figs. 2G–2J). Quenched samples indicate that initial reaction involves dissolution of $Li_2B_4O_7$ and alkali aluminosilicates nearest to this phase, and breakdown of a carbonate (present in some samples) to yield small quantities of CO_2 fluid. By $T >$ 420°C, $Li_2B_4O_7$ crystals had reacted completely with other daughter minerals to yield borosiliciate glass on quench. By 470°C, all traces of crystals were gone in most inclusions, and quench products were glass and aqueous liquid–vapor phases (containing small amounts of CO_2 in samples from the tips of coarse-grained spodumene crystals). The determination of T_m dms in this manner, however, does not indicate whether a single fluid exists in these inclusions above 470°C or two fluids form (silicate-rich aqueous fluid plus hydrous borosilicate melt). If the crystal-rich inclusions represent the unmixed components of a single homogeneous fluid phase (at the point of entrapment), then the observed quench products of borosilicate glass + aqueous fluid also result from exsolution (i.e., the single, homogeneous, hydrous borosilicate fluid is nonquenchable).

The nature of crystal-fluid interaction was observed in part during one unique heating run on the microthermometric stage. In one sample of coarse-grained spodumene, two crystal-rich inclusions (out of hundreds of similar inclusions in several rock chips) persisted at 475°C long enough to observe considerable daughter mineral reaction. The samples were heated from 300 to 475°C at

←

minerals, especially lithium tetraborate (c), show evidence of melting or dissolution, and the vapor bubble is constricted by small amounts of glass (g) that wets the walls of the inclusion. After quench from 425°C (H, partially crossed polars), lithium tetraborate has disappeared completely, most other phases show evidence of appreciable melting or solution, and the vapor bubble is highly distorted by large amounts of glass along the walls of the inclusion. After quench from 450°C (I, partially crossed polars), the crystalline contents have melted or dissolved almost completely to yield borosilicate glass and exsolved aqueous fluid on quench. In most such runs, all traces of crystals are gone after quench from 470°C.

J–M. Types and distributions of inclusions in quartz (reprinted from London, 1985). J. Most samples contain large inclusions with negative crystal forms of quartz; these inclusions are not obviously associated with any fractures (e.g., the inclusions labeled a, which in this case contain H_2O-CO_2 fluids; aqueous Group I inclusions are similar to (a) above). Also present are smaller, rounded to euhedral aqueous inclusions (b) that correspond to Group II aqueous inclusions and define extensively healed fractures, and additional planes of thin, rounded to amoeboid aqueous inclusions (c) that represent the high-salinity Group III aqueous inclusions.

K–M. Photomicrographs of individual inclusions such as those labeled (a) in Figure 2J. Inclusion contents at 25°C are (K) mixed H_2O-CO_2, (L) aqueous, and (M) pure CO_2 (homogenized to liquid). Reprinted from London (1985).

10°C/min, and then held at 475°C for 2 h. Noticeable dissolution of $Li_2B_4O_7$ and cookeite crystals occurred after 30 min; albite crystals showed rounding after 45 min. After 90 min at 475°C, approximately 40 vol% of the $Li_2B_4O_7$ and cookeite and 20 vol% of the albite had dissolved congruently into the aqueous fluid. At approximately 100 min of run time, a separate liquid was observed to coat remnant crystal grains and to move out along the walls of the inclusions. The new liquid was slightly denser than the aqueous liquid (refr. ind. determination by Becke line), but the phase boundary between these two liquids was faint. It is important to note that the denser borosilicate fluid wetted the walls of inclusions and displaced aqueous fluid from the surfaces. By 120 min, grain size of residual crystals was further diminished, and the phase boundary between the coexisting liquids was barely discernible. The run was terminated because of excessive heating of the inclusion stage; upon cooling, the solute-rich aqueous liquid exsolved to glass rubble and (comparatively) low-density aqueous liquid + vapor that was identical to material observed in the quenched hydrothermal runs. Most inclusions that still contained crystals at 470°C were among inclusion clusters that showed evidence of necking down prior to the heating stage and hydrothermal runs.

Coarse-grained spodumene laths and fine-gained spodumene after petalite are cut by fractures delineated by fluid inclusions that postdate the formation of all crystal-rich inclusions described above. The late-stage inclusions have angular to subrounded shapes and variable sizes; at 25°C most consist of aqueous liquid plus vapor. In addition to the general absence of included crystals, they are readily distinguished from the previous inclusion population by their higher salinity and by lower homogenization temperatures (Table 1 and Fig. 1). Where these late-stage fractures cut crystal-rich inclusions, the aqueous contents have been mixed to yield fluids with intermediate salinities and densities.

Minor quantities of relic petalite occur in the quartz–montebrasite–lithium aluminosilicate zone (5) adjacent to a large (upper) body of pollucite (Černý and Ferguson, 1972; Černý, 1975; Crouse et al., 1979). The limited and restricted preservation of petalite raises the question of whether chemical conditions (and hence fluid-inclusion data from petalite) near the pollucite body were representative of the rest of the deposit, in which petalite was completely replaced by spodumene + quartz.

Fluid inclusions in petalite lie along healed fractures and in small planar groups parallel to cleavage {001} (Fig. 2A). Two types of compositionally distinct inclusion clusters are present; both types of inclusions possess variable phase ratios and appear to represent much larger inclusions that have experienced considerable necking down. One population of inclusions consists of low-salinity aqueous liquid plus vapor and crystalline solids (Table 1 and Fig. 2A), which on the basis of the optical and physical similarity to those in spodumene, appear to be albite, cookeite, and $Li_2B_4O_7$. The other type of cluster consists of inclusions with variable proportions of low-salinity H_2O-CO_2 fluids and no included solids (Table 1). The mixed H_2O-CO_2 inclusions lie along fractures as well as the {001} cleavage and thus appear to postdate the crystal-rich inclusions.

An assessment of the inclusion data from petalite is severely limited by the rarity of both samples and fluid inclusions within samples and by obvious postentrapment necking down. It is important to note, however, that some of the observed characteristics of fluids (low salinity) and included solids in the crystal-rich inclusions are similar to those of spodumene, for which many more inclusion data have been obtained.

Quartz

Fluid inclusions were examined in quartz from four associations: (1) intergrown with spodumene as pseudomorphs after petalite, (2) coarse-grained, massive quartz interstitial to large spodumene laths, (3) euhedral smoky crystals from a rare miarolitic cavity, and (4) intergrown with eucryptite as a replacement of spodumene and petalite. Inclusions in quartz intergrown with spodumene after petalite are potentially informative, because the generation of these intergrowths occurred by the isochemical retrograde reaction petalite = spodumene + 2 quartz. Cogenetic spodumene + quartz intergrowths at Tanco formed at some *P-T* conditions on or near this reaction boundary, which has been located in the *P-T* plane by reversed phase-equilibrium experiments (London, 1984a). Černý (1972b, 1975) identified small amounts of eucryptite associated with spodumene + quartz pseudomorphs of petalite, and with some relic petalite, near the upper pollucite body. Fluid inclusions in eucryptite + quartz could be used in the same manner as spodumene + quartz assemblages, because the stability field of eucryptite + quartz is bounded by a pressure-dependent reaction involving spodumene and a temperature-sensitive reaction with petalite (London, 1984a). At Tanco, however, the eucryptite + quartz intergrowths may contain at least two generations of quartz: one produced by the breakdown of petalite and a later generation by retrograde breakdown of spodumene. Moreover, it is not possible to distinguish quartz from eucryptite in the polished chips. Massive quartz intergrown with coarse-grained laths of spodumene is typical of the quartz-rich interior zones. Miarolitic cavities are rare at Tanco; however, one such pocket in the microcline–quartz–lithium aluminosilicate zone (4 of Crouse et al., 1979) provided euhedral smoky quartz crystals for this study.

Inclusion contents and microthermometric properties are remarkably similar in all types of quartz (except quartz with eucryptite; inclusions in eucryptite + quartz intergrowths are discussed separately below). Inclusions hosted by quartz differ from inclusions in spodumene in three important respects: (1) most inclusions contain only liquid and vapor phases at 25°C; crystalline solids are generally absent; (2) they are comparatively CO_2-rich, and many

contain pure CO_2; and (3) the aqueous component is comparatively saline (as determined by ice disappearance in aqueous inclusions and clathrate disappearance in mixed H_2O-CO_2 inclusions).

There are three compositionally distinct types of inclusions in quartz (Figs. 2J–2M): (1) mixed H_2O-CO_2 inclusions that contain an average 5–15 mol% CO_2 (determined from visual estimates of phase volumes at 25°C and from calculated volumes using the method of Bodnar, 1983); (2) aqueous inclusions with no CO_2; and (3) essentially pure CO_2 inclusions with little or no H_2O. Fields of inclusions with highly variable H_2O/CO_2 do occur but are not abundant in the samples analyzed to date.

Shapes, sizes, and distributions of inclusions are variable but show some consistencies among all types of quartz. Mixed H_2O-CO_2 inclusions are large (most are 30–50 μm), possess rounded to sharp negative crystal forms of the host quartz, and tend to be (or appear) randomly distributed (i.e., show no tendency for planar clustering or alignment; see Fig. 2J). Pure-CO_2 inclusions possess similar shapes and distributions but are smaller (15–30 μm). Aqueous inclusions show the widest ranges in size (2–200 μm), shape (amoeboid to negative crystal forms), and distribution (large, isolated inclusions to planar arrays of rounded or amoeboid individuals).

In the following discussion, inclusions are grouped on the basis of composition, because the types and properties of inclusions in quartz from most associations are so similar. The microthermometric data for each inclusion type in each association are given in Table 1.

Mixed H_2O-CO_2 inclusions. Inclusions with uniform H_2O/CO_2 are present in all quartz except that associated with eucryptite (where X_{CO_2} varies from approximately 0 to 1 among inclusion clusters). In general, these are the largest, most regularly shaped (negative crystals forms), and most widely dispersed of all inclusion types (e.g., Fig. 2J). Visual estimates of phase proportions at 25°C indicate that these inclusions in massive and miarolitic quartz contain approximately 15–25 vol% CO_2, and in quartz associated with the pseudomorphs after petalite, approximately 20–40 vol% CO_2. The proportion of H_2O/CO_2 varied by several volume percent between samples but was consistent among large numbers of inclusions within a given specimen. Estimates of phase proportions were subsequently checked by the method of Bodnar (1983).

Clathrate-disappearance temperatures in mixed H_2O-CO_2 inclusions (Table 1 and Fig. 1) yield calculated salinities equivalent to 8.0(0.1)[86] and 8.5(0.1)[88] wt% NaCl in miarolitic and massive quartz, respectively, and slightly higher and more variable salinity (10.5(5.0)[36] wt% NaCl) in quartz of pseudomorphs after petalite (Table 1 and Fig. 1).

Homogenization of CO_2 liquid and vapor ranges from +18° to +29°C in inclusions that contain a visible aqueous phase (liquid that wets the walls of inclusions) at near-room temperatures. Measurements of T_h LV CO_2 in mixed H_2O-CO_2 inclusions were not routinely recorded because such measurements provide density information that is pertinent only to conditions near T_h LV CO_2 (i.e., the H_2O phase that surrounds CO_2 is compressible relative to the rigid walls of the inclusion). T_h LV CO_2 was measured for pure-CO_2 inclusions only, because isochoric extrapolations from these data provide meaningful estimates of the densities of exsolved CO_2 liquids at the conditions of pegmatite formation.

Upon heating, approximately 85–95% of mixed H_2O-CO_2 inclusions in massive and miarolitic quartz, respectively, undergo complete homogenization prior to decrepitation. In quartz from pseudomorphs after petalite, almost 50% of observed inclusions decrepitate prior to final homogenization; such behavior is consistent with higher solvus temperatures and higher internal fluid pressures as a result of higher CO_2 content and salinity. Those inclusions that did not decrepitate homogenized to H_2O-rich liquid between 280 and 290°C [181] (Table 1 and Fig. 1). The CO_2 content of inclusions that homogenized was checked (albeit by circular reasoning) by the phase-volume method of Bodnar (1983). From clathrate-disappearance temperatures and visual estimates of CO_2 content, the composition of the homogeneous fluid can be expressed as approximately 91 mol% H_2O, 5 mol% CO_2, and 4 mol% NaCl equivalent. The density of this fluid at the mean T_h LV (285°C) is 0.95(0.01) g/cm^3 (cf. Fig. 2C of Bowers and Helgeson, 1983b). With this final average density, the volumes of inclusion contents can be calculated from the method of Bodnar (1983); by this technique, the calculated proportion of CO_2 liquid (at 29°C, after liquid-vapor homogenization of CO_2) is 19 vol% (= 6 mol%). The uniformity of phase proportions, salinities, and homogenization temperatures among large numbers of these inclusions suggests that the entrapped fluid was a homogeneous phase that was widely dispersed throughout the pegmatite.

Aqueous inclusions. All quartz at Tanco contains aqueous inclusions with no CO_2; these inclusions exhibit a wide range of shapes, sizes, and compositions (as reflected by microthermometric measurements). Where possible, the aqueous inclusions have been subdivided into groups on the basis of apparent sequence of entrapment as indicated by crosscutting relationships of inclusion-filled fractures. In massive quartz interstitial to coarse-grained spodumene, three distinct groups were recognized. In quartz from other associations, distinctions on the basis of microthermometric properties and crosscutting relations were less obvious (to the point that there was no justifiable rationale for separation of aqueous inclusions in quartz associated with pseudomorphs after petalite, as discussed under Interpretation of Inclusion Data). Group I inclusions are the largest (average 15–30 μm), most regularly shaped, and most widely dispersed (Fig. 2K); Group II inclusions have variable size and shape, but most lie along recognizable cracks; Group III inclusions are generally smallest (5–20 μm), most irregular in shape, and lie along well-defined, late-stage fractures (Fig. 2J). From an assessment of distribution and microthermometric properties presented below, the large, euhedral,

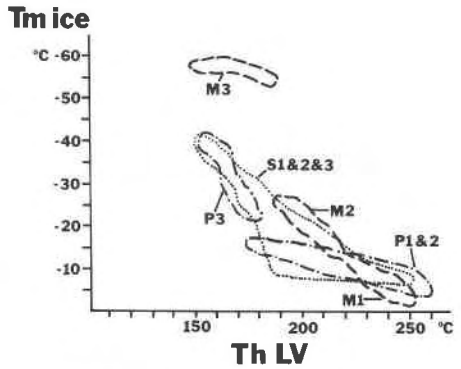

Fig. 3. Range of variation of salinity (T_m ice) with T_h LV for aqueous inclusions in quartz. M: massive quartz interstitial to spodumene, Group I (M1, $N = 32$), Group II (M2, $N = 53$), and Group III (M3, $N = 59$). P: quartz from a miarolitic pocket, Groups I and II (P1&2, $N = 163$) and Group III (P3, N = 30). S: spodumene + quartz pseudomorphs after petalite, all inclusions (S1&2&3, $N = 97$).

dispersed inclusions with lowest salinities and highest homogenization temperatures (Group I) appear to have been trapped first (i.e., at highest P and T), followed by inclusions that show progressive change from large to small, euhedral to rounded to amoeboid shapes, dispersed to planar clustering, increasing salinities and decreasing homogenization temperatures, with sequentially later entrapment (Groups II and III).

Eutectics of all aqueous inclusions are lower than those in spodumene and petalite, and apparent salinities are higher (Fig. 1). Eutectics decrease from −48°C in Group I (massive quartz) to −100°C in Group III (massive quartz) (Table 1). Similarly, T_m ice in aqueous inclusions decreases from Group I to Group III. Average values of T_m ice (−7.2 to −57.7°C) correspond to equivalent salinities as low as 10.7 wt% NaCl for Group I to 61.7 wt% NaCl for Group III. Crystalline solids, however, are rare in all aqueous inclusions in Tanco quartz; thus, the solutions even those with extremely low T_m ice in Group III, are generally undersaturated with respect to any solute phase. Examination of opened inclusions by SEM revealed rare crysals of halite and epsomite (?). Salinities of the aqueous inclusions in quartz clearly increase with decreasing T_h LV (Fig. 3).

Consistent and significant differences in T_h LV were observed where inclusion populations could be sorted (e.g., as in massive quartz). Group I inclusions possess the highest average T_h LV = 205 to 213°C (Table 1), and Group III the lowest average T_h LV = 139°C. Many such inclusions (especially the largest ones) leak by partial decrepitation prior to total decrepitation, and some inclusions exhibit partial decrepitation prior to homogenization (London, 1985); thus, care was taken during heating runs to measure T_h LV only in those inclusions in the immediate field of view, and to heat chips only once.

Pure-CO_2 inclusions. Inclusions that appear to contain only CO_2 liquid and vapor at 25°C (Fig. 2M) are present in all quartz samples but are abundant only in quartz associated with spodumene after petalite. In these inclusions (in quartz of pseudomorphs after petalite), $T_e = T_m$ $CO_2 = -56.9(0.3)$°C [58] (Fig. 1 and Table 1). Within the limits of calibration and thermocouple uncertainty, this fluid does not appear to contain significant amounts of any other components (e.g., CH_4 or N_2). Homogenization temperatures in pure-CO_2 inclusions cover a wide range (T_h LV = −2°C to +22°C), but the standard deviation about the mean is comparatively low (5.6(3.7)°C [264], Table 1).

Inclusions in eucryptite + quartz. Inclusions in this assemblage (both quartz and eucryptite) possess angular, irregular shapes, variable sizes, and lie along healed fractures. Highly variable phase proportions among inclusion clusters bear evidence of extensive liquid-vapor phase separation prior to or during healing (necking down) of fractures. Included crystalline solids are more common than in fluid inclusions hosted by quartz in other associations; however, the distribution of included solids is variable and does not clearly indicate a daughter-mineral assemblage (cf. spodumene).

Eutectics and final melting temperatures of solid CO_2 are close to the CO_2 triple point (Table 1 and Fig. 1). Inclusions that appear to contain pure CO_2 homogenize at a higher average temperature than comparable inclusions in quartz from petalite pseudomorphs (Table 1).

In aqueous inclusions, values of T_e, T_m ice, and T_h LV are similar to those of quartz-hosted inclusions in other associations, except that the homogenization data from eucryptite + quartz intergrowths are more dispersed and have a lower mean value (Table 1 and Fig. 1). The aqueous inclusions could not be meaningfully divided into different populations on the basis of shape, size, or crosscutting relationships. In eucryptite + quartz, microthermometric properties of individual planar clusters cover the range of the entire population of inclusion type.

Interpretation of inclusion data

Spodumene and petalite

The uniformity of the crystalline phase assemblage and of liquid-crystal phase proportions in the crystal-rich inclusions leads to two important interpretations: (1) the included solids are daughter minerals and hence represent an important component of the entrapped fluid and (2) the daughter minerals plus aqueous fluid represent the products of a single homogeneous phase (Table 2). Consistency of phase proportions is crucial to this interpretation, and not all inclusion clusters exhibit the uniformity pictured in Figure 2. In a preliminary report of this work (London, 1982; London et al., 1982), the variable crystal/liquid ratios in some inclusion clusters were taken as possible evidence for entrapment of variable proportions of coexisting (i.e., immiscible) H_2O-rich and silicate-rich fluids. As a result of more complete study, including recognition of large inclusion clusters with uniform crystal/liquid proportions and phase assemblages such as those in Figure 2B, together with preliminary experimental data discussed below, the variations in crystal/liquid contents

are now regarded as the result of necking down of large inclusions after most or all daughter minerals had been deposited from solution. If this interpretation is correct, then the homogeneous fluid phase (hydrous borosilicate liquid, now represented by crystal-rich inclusions such as those in Figs. 2C, 2D) is a sample of the pegmatite fluid that wetted petalite crystal surfaces during growth and subsequent pseudomorphism, and may have been the *only* fluid phase in the pegmatite system at that time (at least, it did not coexist with the comparatively low-density, solute-poor, CO_2-bearing fluids represented by many inclusions in quartz) (London, 1984b). The last statement cannot be verified from the quench products of hydrothermal homogenization runs alone. Additional support for this interpretation comes from reconnaissance experiments in the model system $LiAlSiO_4$-$NaAlSi_3O_8$-SiO_2-$Li_2B_4O_7$-H_2O at P_{fluid} = 2 kbar (London, 1983).

System $LiAlSiO_4$-$NaAlSi_3O_8$-SiO_2-$Li_2B_4O_7$-H_2O. Experiments in this system were intended to test the validity of the interpretations made from the inclusions in Tanco spodumene, and to quantify the effects of $Li_2B_4O_7$ on liquidus phase relations and solubilities in alkali aluminosilicate systems at elevated P_{H_2O}. Reactants were reagent-grade $Li_2B_4O_7$, natural albite (Amelia, Virginia), eucryptite (Bikita, Zimbabwe), quartz (Minas Gerais, Brazil), and distilled and deionized water. Charges were sealed in 1-cm Pt capsules for runs in conventional cold-seal hydrothermal vessels. Liquidus temperatures for 30 different bulk compositions in borate-rich portions of the system ($Li_2B_4O_7$ > 10 wt% solids) were located first by melting reactions with increasing temperature and then were reversed by runs undercooled from supraliquidus temperatures. Phase relations on the liquidus are not totally resolved (Fig. 4); undercooling experiments yielded several unidentified phases (probably metastable Li silicates and borates). Nevertheless, five important conclusions can be derived from the existing data: (1) addition of $Li_2B_4O_7$ lowers the solidus of this system to 500°C at P_{fluid} = 2 kbar; (2) crystallization of lithium aluminosilicates (petalite + quartz + albite, and petalite + eucryptite + albite) drives the liquid composition toward the middle of the $NaAlSi_3O_8$-$Li_2B_4O_7$ join (Fig. 4); (3) addition of $Li_2B_4O_7$ leads to extensive silicate liquid–H_2O miscibility that approaches or attains complete miscibility (as predicted by Pichavant, 1983, but at lower concentrations of B_2O_3) toward minimum melt compositions; (4) addition of $Li_2B_4O_7$ greatly enhances rates of crystal growth; euhedral, nonskeletal crystals of quartz, albite, and petalite grew to dimensions of 0.5 mm in runs of 72-h duration; and (5) addition of $Li_2B_4O_7$ leads to extreme reductions in melt viscosity, presumably through melt depolymerization and increased H_2O solubility. In runs at liquidus temperatures, crystals of quartz, albite, and petalite settled to the bottom of charges (within quenched glass beads) to form grain-contact cumulates in runs of 48 h or less, depending on bulk composition; solution of the Stokes equation yields crude viscosity estimates of 10^2 poise (probably correct within one order of magnitude). It should be noted that all of these runs that produced large, euhedral crystals in 48–72 h were vapor-undersaturated (i.e., the borosilicate liquid could not be saturated with respect to H_2O); thus, coarse grain size and idiomorphic forms should not be construed as unequivocal evidence for the existence of an exsolved aqueous phase.

Table 2. Approximate contents of inclusions in spodumene (coarse laths and pseudomorphs after petalite)

Phase	Vol %	density, g/cc	wt %
aqueous fluid	50	0.75**	22.1
albite	30	2.61	46.6
pollucite	5	2.90	8.6
cookeite	5	2.67	7.9
$Li_2B_4O_7$	10	2.43	14.5

Estimated Bulk Composition*

Component	wt %
Li_2O	2.8
Na_2O	5.5
Cs_2O	3.7
Al_2O_3	14.3
SiO_2	37.9
B_2O_3	12.0
H_2O	23.8

* does not include (1) up to 5 vol % of carbonate that is present in some inclusions in coarse-grained spodumene, and (2) dissolved contents of aqueous fluid.
** calculated from microthermometric properties

The model system is clearly not a perfect analogue to the Tanco inclusion contents, because the natural fluid from Tanco contains appreciable amounts of Cs and other components. Like the synthetic system in which molecular proportions of alkalis/aluminum > 1, however, the Tanco liquid is mildly peralkaline [molecular $(Li_2O + Na_2O + Cs_2O)/Al_2O_3$ = 1.36, from Table 2] in spite of the presence of the peraluminous phase cookeite in fluid inclusions. At such high alkali/aluminum proportions, B should be largely in fourfold coordination in the fluid or melt at P-T conditions of entrapment (cf. Bray, 1978; Konijnendijk and Stevels, 1978; Pichavant, 1983). Several points are directly applicable to the natural Tanco system. The crystallization sequence and liquid line of descent of the synthetic system are similar to those of the Tanco pegmatite (alkali borosilicate liquid hosted by lithium aluminosilicate + quartz assemblages, with subsequent crystallization of silica-undersaturated phases such as eucryptite and analcime plus albite). The results imply that $Li_2B_4O_7$ concentrations comparable to those of the Tanco inclusions are capable of extreme depression of alkali aluminosilicate solidi (especially at elevated H_2O pressures), and of depression of the solvus of silicate liquid + H_2O vapor to the point that these fluid components are completely miscible at geologically feasible P-T conditions. The extensive reciprocal solubilities of silicate and aqueous components observed in the experimental studies

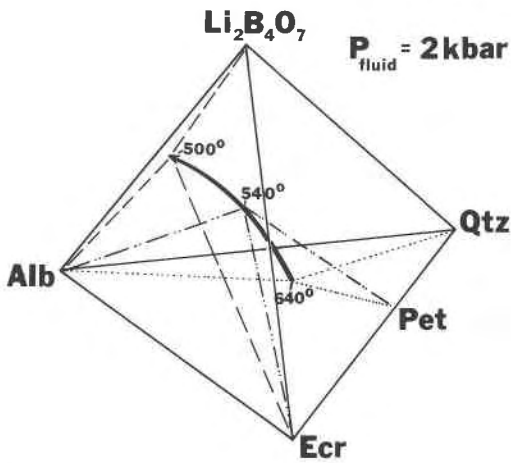

Fig. 4. Preliminary phase relations in the system $LiAlSiO_4$ (Ecr)–$NaAlSi_3O_8$ (Alb)–SiO_2 (Qtz)–$Li_2B_4O_7$–H_2O at P_{fluid} = 2 kbar, showing the liquid line of descent and apparent stable crystalline assemblages (connected by tie lines to liquid compositions at approximate T). All bulk compositions of this study contained >10 wt% $Li_2B_4O_7$; phase relations on the Alb-Qtz-Ecr plane are from Stewart (1978).

imply that if two separate fluids did coexist, their densities and perhaps their compositions probably were quite similar. The general lack of evidence for entrapment of two immiscible fluid phases by Tanco spodumene appears to signify that only one hydrous alkali borosilicate fluid existed at that point in the evolution of the pegmatite; it is possible, however, that the high content of alkali borate component could have caused immiscibility between two silicate-rich liquids.

In the reconnaissance experiments described above, runs quenched from supraliquidus temperatures along the SiO_2-$Li_2B_4O_7$ join yielded opalescent glasses over a compositional range of approximately 60–80 wt% SiO_2 (excluding the weight fraction of H_2O). Liquid immiscibility (manifest by opalescence of quenched glasses) between B_2O_3-SiO_2 and especially alkali borate–SiO_2 has been documented in anhydrous and some hydrous systems (e.g., Morey, 1951; Rockett and Foster, 1965, 1966; Charles and Wagstaff, 1968; Pichavant, 1981, 1983; Hervig and Navrotsky, 1985). Liquid immiscibility between alkali borosilicate and silica-rich fluids represent a possible explanation for the generation of essentially pure quartz cores in boron-rich pegmatites, and for the immediate proximity of massive quartz bodies and tourmaline-bearing albitites at Tanco and numerous other localities (e.g., see Fig. 8 of Černý and Ferguson, 1972, and Fig. 97 of Černý et al., 1981). The sharpness of these contacts and their smooth, sometimes sinusoidal to convoluted boundaries are suggestive of a liquid-liquid interface; traditionally, such contacts have been interpreted as the result of subsolidus albitization of massive quartz cores (e.g., Beus, 1960; Černý et al., 1981), or of thermally and gravitationally induced chemical gradients in a magma that is exsolving an aqueous phase (e.g., Jahns and Tuttle, 1963; Jahns, 1982). The sharpness of albitite–massive quartz contacts, however, appear to preclude the last hypothesis as a viable mechanism. In present exposures of albitite–quartz core contacts at Tanco, teardrop-shaped masses of albitite are suspended in massive quartz, and some layered aplites have been gently deformed and ripped up (but not brecciated), with infilling of voids by massive quartz. These features appear to indicate that the fluids that formed the albitites and quartz cores coexisted and that the liquid that crystallized to form the quartz core was sufficiently dense and viscous that it could suspend blobs and rafted layers of albitite. The possibilities of liquid immiscibility are especially pertinent to this study, because petalite and spodumene crystals, which host the inclusions that are interpreted as entrapped alkali borosilicate fluid, are themselves embedded in massive quartz, not in tourmaline-bearing albitite. If silica–alkali borosilicate immiscibility did exist, then it can be inferred that the alkali borosilicate fluid wetted the surfaces of growing petalite and spodumene crystals. Again, there is field evidence at Tanco and elsewhere that is suggestive of this process: albite-mica assemblages—commonly with tourmaline, beryl, apatite, and Nb-Ta oxides—rim unresorbed spodumene or petalite crystals that are embedded in massive quartz (e.g., at Harding, New Mexico; White Picacho district, Arizona; Middletown district, Connecticut; Rumford-Newry district; Maine; and many other localities). Furthermore, in the fluid-inclusion homogenization runs described above, the borosilicate liquid generated in spodumene-hosted inclusions wetted the inclusion walls and displaced aqueous fluid from the surface.

The apparent presence of a lithium or beryllium carbonate daughter mineral adds another component to the hydrous borosilicate fluid. This phase is optically similar to $Li_2B_4O_7$ in polished chips, except that where the two phases are present in the same inclusion, the carbonate clearly displays higher birefringence and higher relief (Fig. 2C). The presence of the carbonate is manifest by daughter-mineral homogenization runs that liberate CO_2 fluid. On the basis of the crystal homogenization runs, the carbonate appears to be most abundant in inclusions near the ends of large spodumene crystals, presumably the latest spodumene to grow during cooling of the Tanco system. This carbonate is the probable source of CO_2 fluid that appears in fluid inclusions in quartz. Addition of a lithium or beryllium carbonate should further reduce solidus temperatures (cf. Koster van Groos and Wyllie, 1966); however, there are no pertinent experimental data on which to base a comparison of the effects of lithium borate versus lithium or beryllium carbonate on fluid composition and properties at elevated P_{H_2O}. From the crystal-homogenization runs, the carbonate component appears to be subordinate to $Li_2B_4O_7$, even within the most carbonate-rich inclusions (n.b.: Foord et al. (1986) have reported borates and carbonates from miarolitic pockets of the gem-bearing Himalaya dike, California).

Conditions of fluid entrapment. The hydrous borosilicate liquid was presumably present and entrapped by

spodumene (and petalite) at P-T conditions on or near the petalite-spodumene-quartz reaction boundary. Hydrothermal homogenization runs put the minimum entrapment temperature at 470°C, which by extrapolation to the univariant reaction boundary establishes a minimum pressure at 2700 bars (Fig. 5A). These conditions may be near the actual temperature and pressure at entrapment. At the point of petalite replacement, the Tanco pegmatite was undoubtedly saturated with respect to quartz and albite, both of which are daughter minerals within the inclusions. The entrapped fluid would precipitate quartz and albite shortly after inclusion closure, because the pegmatite system was on a liquidus surface; 470°C is the liquidus temperature for the bulk composition of the inclusion contents. Notice in Figure 5A that extrapolation of the aqueous fluid isochore to the range of T_m dms yields minimum P-T conditions that are consistent with entrapment at 470°C and 2700 bars. The extrapolation of the aqueous-liquid isochore to the interval of T_m dms may not be strictly valid; although the inclusion volume remains constant to near 375°C, above this temperature, inclusion volume increases and fluid density may change as daughter minerals melt or dissolve. In spite of this, extrapolation of the aqueous-fluid isochore through the interval of T_m dms may be justifiable for two reasons: (1) isochores for aqueous fluids of significantly different densities are essentially coincident in this P-T region (Fig. 8 of Roedder and Bodnar, 1980) and (2) isochores for hydrous albite melt are not substantially different from the slope of the isochore for the aqueous liquid in spodumene-hosted inclusions (cf. Fig. 8 of Burnham and Davis, 1971).

Quartz

Inclusions in quartz (plus eucryptite) from four paragenetic associations in the pegmatite are fundamentally similar but obviously different from those in spodumene. An interpretation of these inclusions and their relationships to those in spodumene are based on a combination of microthermometry, inclusion size, shape, and crosscutting relationships of planes of inclusions, and constraints on the P-T path of the pegmatite as defined by reaction relationships among lithium aluminosilicates.

From point B of Figure 5A, the trajectory of the cooling path must have approached and entered the field of eucryptite + quartz. With this constraint, the conditions of fluid evolution and entrapment in quartz can be ascertained by examination of the sequence in which fluid isochores are intersected, and by crosscutting relationships of compositionally different populations of fluid inclusions. It must be reiterated, however, that the isochores shown in Figure 5 are approximations that are especially poor for the high-salinity aqueous liquids, for which the system H_2O-NaCl is not a valid analogue to the natural aqueous fluids at Tanco.

The first isochore to be crossed is that of the mixed H_2O-CO_2 inclusions (Fig. 5B). These inclusions appear to represent a CO_2-bearing aqueous fluid that was widely distributed throughout the pegmatite; the CO_2 fluid probably was generated by the breakdown of the carbonate component that is now manifest as a daughter mineral in the inclusions in spodumene. The salinity of this CO_2-bearing aqueous fluid is higher than that of the aqueous component of inclusions in spodumene, but lower than that of the aqueous (CO_2-absent) inclusions in quartz. Despite uncertainties, isochores of aqueous inclusions fall on the low P-T side of the isochore for the mixed H_2O-CO_2 inclusions (Fig. 5C). The most plausible explanation of these relations is to consider the aqueous inclusions, plus pure-CO_2 inclusions, as the products of an unmixed H_2O-CO_2-salt system; the contents of the mixed H_2O-CO_2 inclusions in quartz appear to represent a homogeneous fluid that existed in the pegmatite prior to solvus intersection. If this interpretation is correct, then the solvus would have to lie between the point of intersection of the cooling path with the H_2O-CO_2 isochore (point D, Fig. 5B), and the region of intersection of the isochores for pure-CO_2 and aqueous inclusions (near point F, Fig. 5C). Mixed H_2O-CO_2 inclusions with comparably high CO_2 contents and higher salinities have been noted in most types of quartz, especially in pseudomorphs after petalite. Although these inclusions decrepitate prior to homogenization, their compositions (from clathrate-disappearance temperatures and visual estimates of phase volumes at 25°C) are estimated to be approximately 80–85 mol% H_2O, 10–15 mol% CO_2, and 5–6 mol% NaCl equivalent. The solvus for such a fluid (point E, Fig. 5B) lies approximately within the P-T range between the mixed H_2O-CO_2 isochore (D, Fig. 5B) and the area of intersection of the aqueous and pure-CO_2 isochores (E, Fig. 5C) (see Bowers and Helgeson, 1983b). Thus, there is some inclusion evidence to suggest that CO_2 and salt contents of the homogeneous fluid increased slightly but sufficiently to cause unmixing in the P-T region between isochores as defined above. One problem with this interpretation is that it requires essentially no miscibility between H_2O and CO_2 (i.e., the generation of pure-CO_2 inclusions and CO_2-absent aqueous inclusions) at relatively high P and T, whereas calculated and experimental data for the system H_2O-CO_2-NaCl indicate that there should be significant H_2O-CO_2 miscibility at these conditions (and thus observable as unmixed fluids at 25°C) (e.g., Bowers and Helgeson, 1983a). As noted above, however, the system H_2O-CO_2-NaCl may not be a satisfactory analogue to the Tanco fluid.

Mixed H_2O-CO_2 inclusions with uniform H_2O/CO_2 do not occur in the eucryptite + quartz intergrowths, and this is consistent with H_2O-CO_2 unmixing (solvus intersection) at P-T conditions well beyond the stability field of eucryptite + quartz. As a whole, the aqueous components of inclusions in these intergrowths possess salinities that are comparable to those of Groups II and III in quartz from the other associations; the absence of low-salinity fluids (comparable to those of mixed H_2O-CO_2 and Group I aqueous inclusions in other types of quartz) constitutes further evidence that the salinity of the aqueous-fluid

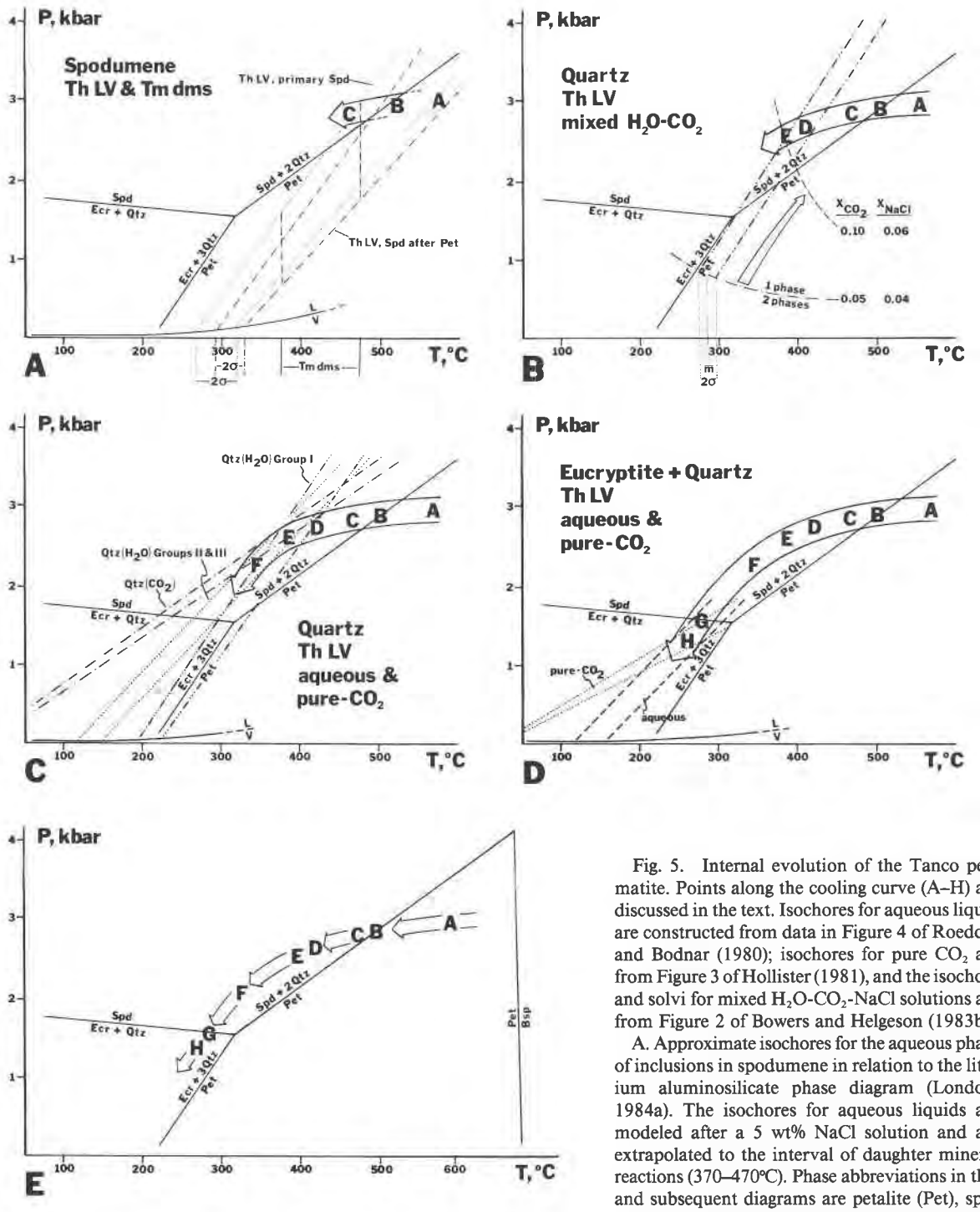

Fig. 5. Internal evolution of the Tanco pegmatite. Points along the cooling curve (A–H) are discussed in the text. Isochores for aqueous liquid are constructed from data in Figure 4 of Roedder and Bodnar (1980); isochores for pure CO_2 are from Figure 3 of Hollister (1981), and the isochore and solvi for mixed H_2O-CO_2-NaCl solutions are from Figure 2 of Bowers and Helgeson (1983b).

A. Approximate isochores for the aqueous phase of inclusions in spodumene in relation to the lithium aluminosilicate phase diagram (London, 1984a). The isochores for aqueous liquids are modeled after a 5 wt% NaCl solution and are extrapolated to the interval of daughter mineral reactions (370–470°C). Phase abbreviations in this and subsequent diagrams are petalite (Pet), spodumene (Spd), eucryptite (Ecr), quartz (Qtz), and β-spodumene (Bsp).

B. Approximate isochore for mixed H_2O-CO_2 inclusions in all samples of quartz. The arrow shows the change in solvus position with increasing salinity and CO_2 from a fluid composition of 91 mol% H_2O, 5 mol% CO_2, 4 mol% NaCl, to 84 mol% H_2O, 10 mol% CO_2, 6 mol% NaCl.

C. Isochores for all aqueous and pure-CO_2 inclusions in quartz. Isochores for saline aqueous inclusions (Groups II and III) are modeled after a 25 wt% NaCl solution, but are approximate because of a lack of relevant *P-V-T* data.

D. Isochores for aqueous and pure CO_2 inclusions in eucryptite + quartz.

E. The cooling path of the Tanco pegmatite.

component increased with decreasing P and T during the crystallization of Tanco. There are some mixed H_2O-CO_2 inclusions, but their phase proportions are extremely variable and they appear to be the products of necking down in an extensively unmixed two-phase system. Pure-CO_2 and CO_2-absent aqueous inclusions represent the compositions of immiscible liquids present during or after formation of eucryptite + quartz. The area of intersection of isochores for these two liquids (i.e., after liquid-vapor homogenization within respective inclusion types) lies just below the eucryptite + quartz = spodumene reaction boundary (Fig. 5D).

Inclusions in pseudomorphs after petalite

Isochemical breakdown of petalite has produced intergrowths of cogenetic spodumene + quartz. The properties of crystal-rich inclusions in spodumene are consistent with fluid entrapment at P-T conditions along the stable portion of this reaction boundary. Thus, these inclusions are regarded as primary and representative of the fluid medium that wetted the surfaces of petalite crystals during primary growth and subsequent pseudomorphism. In contrast, inclusions in quartz of the pseudomorphs possess markedly different compositions, and all feasible estimates of their entrapment conditions fall within the spodumene stability field at P and T below the univariant reaction boundary. Moreover, experimental evidence in the system $LiAlSiO_4$-$NaAlSi_3O_8$-SiO_2-$Li_2B_4O_7$-H_2O implies that for bulk compositions similar to those of the spodumene-hosted inclusions, a hydrous borosilicate liquid and a separate aqueous fluid with low solute concentrations cannot coexist; the two fluids would be extensively if not completely miscible. Thus, the fluid represented by inclusions in spodumene did not coexist with the fluids entrapped by quartz. There is no evidence that quartz ever entrapped samples of the fluid that was present during petalite replacement; solid inclusions, with or without associated fluid, are virtually absent in Tanco quartz. From isochoric extrapolations, the fluids represented by inclusions in quartz were generated at lower P and T than those in spodumene and could only have been generated after the borosilicate fluid had evolved through crystallization to the comparatively solute-poor, CO_2-bearing aqueous fluid. Therefore, inclusions in quartz of petalite pseudomorphs are secondary in that they are not representative of the fluid medium and P-T conditions of petalite pseudomorphism (however, similar inclusions in miarolitic quartz and eucryptite + quartz intergrowths could be primary). An important conclusion for fluid-inclusion research is that examination of inclusions in only quartz would lead to an erroneous interpretation of the fluid properties and P-T conditions during petalite replacement. Some additional arguments for a secondary origin for these inclusions and implications for the use of inclusions in quartz from pegmatites and related magmatic-hydrothermal systems are discussed elsewhere (London, 1985).

Internal evolution of the Tanco pegmatite

The combination of fluid-inclusion data and lithium aluminosilicate reaction relationships elucidates in detail the cooling path and crystal-fluid evolution during the middle to late stages of pegmatite consolidation, the poorly defined "pneumatolytic" transition from magmatic to hydrothermal conditions. The following synopsis of events is depicted graphically in Figure 5E.

Saturation with respect to primary petalite occurred below 680°C and 4100 bars, the upper P-T limits of the petalite + quartz stability field; conditions of about 600°C and 3250 bars constitute a reasonable estimate for petalite saturation (point A, Fig. 5E). Upon cooling, the pegmatite intersected the univariant petalite = spodumene + 2 quartz reaction boundary at approximately 500°C and 2900 bars (point B, Fig. 5E), whereupon petalite was replaced isochemically by spodumene + quartz intergrowths, and spodumene succeeded petalite as the stable primary lithium aluminosilicate; growth of primary spodumene continued to 470°C and 2700 bars (point C, Fig. 5E). Primary growth and subsequent replacement of petalite, and continued crystallization of primary spodumene, took place in the presence of a dense, hydrous alkali borosilicate fluid (Table 2) in which H_2O may have been completely miscible. The CO_2 content of the borosilicate fluid apparently increased with progressive fractional crystallization, as indicated by the increasing amounts of lithium or beryllium carbonate daughter mineral in inclusions toward the ends of large spodumene crystals.

The high alkali borate content of the pegmatitic fluid may have promoted silica–alkali borosilicate liquid immiscibility that led to crystallization of massive quartz cores and adjacent albitites that are separated by smooth, razor-sharp, and undulatory contacts. This interpretation is supported by the limited experimental data on alkali borate–silicate liquidus relations, and by observations of textures at Tanco and elsewhere. If correct, this hypothesis could account for the noneutectic compositions (with respect to the haplogranite system) and roughly contemporaneous crystallization of essentially monomineralic quartz and feldspar zones (e.g., Jahns, 1982; Walker, 1985; Jolliff et al., 1986).

By 420°C and 2600 bars (point D, Fig. 5E), the fluid phase had changed significantly to a solute-poor, CO_2-bearing homogeneous aqueous fluid with the approximate composition 91 mol% H_2O, 5 mol% CO_2, and 4 mol% NaCl equivalent. With slight increases in CO_2 and salinity, nonideal mixing led to H_2O-CO_2 immiscibility (solvus intersection) at about 390°C and 2500 bars (point E, Fig. 5E); the composition of the fluid at the point of solvus intersection may have been approximately 80–85 mol% H_2O, 10–15 mol% CO_2, and 5–6 mol% NaCl equivalent. Between 390 and 300°C and between 2500 and 1800 bars, the H_2O-CO_2-salt system unmixed completely to an essentially pure-CO_2 liquid that coexisted with a comparatively saline aqueous liquid (point F, Fig. 5E). The density and salinity of the coexisting aqueous liquid increased

with decreasing P and T (Fig. 3). The Tanco pegmatite entered the stability field of eucryptite + quartz at approximately 280°C and 1600 bars (points G and H, Fig. 5E); at such low temperatures, the breakdown of spodumene and minor relic petalite to eucryptite + quartz apparently was sluggish so that the retrograde replacement was incomplete. Fluid-inclusion data from the amoeboid inclusion clusters with widely varying phase ratios and microthermometric properties bear evidence of the diminished efficacy of fracture healing and recrystallization at low temperatures in the eucryptite + quartz field.

Following unmixing of H_2O and CO_2 below 390°C and 2500 bars, the salinities (and CO_2 contents?) of H_2O-rich fluids increased with degree of crystallization and with decreasing P and T at subsolidus conditions. Microthermometric data reflect increasing solute complexity in the evolving fluid with little or no saturation in any one phase. A general increase in salinity and CO_2 content might be caused by devolatilization of residual silicate-rich fluids, from subsolidus hydration reactions (e.g., as in the extensive production of secondary Li-micas at Tanco), or by mixing with more saline and CO_2-rich fluids from outside the pegmatite. Variations in the extent of subsolidus replacement and in the composition of the replaced phase (e.g., microcline, pollucite, or lithium aluminosilicates) may have contributed to local differences in salinity and solute species (cf. London and Burt, 1982a, 1982c). The salinity variations, however, are distinctly polymodal, and given the large number of inclusions that were examined, it is unlikely that this distribution results from incomplete sampling. Polymodal distributions could result from sporadic entrapment (i.e., episodic fracturing of quartz) of a continuously evolving fluid, or from discontinuous changes in the pegmatite-fluid composition (e.g., from mixing with fluids derived from the pegmatite wall rocks). Oxygen- and hydrogen-isotype systematics, however, do not indicate a significant influx of host-derived fluids at Tanco or at other similar rare-element pegmatites (Taylor and Friedrichsen, 1983; Walker, 1985).

The *P-T* path

Allowing for minor uncertainties in curvature and inflection, the combination of fluid-inclusion data with lithium aluminosilicate reaction relationships defines the cooling path of the Tanco pegmatite from about 600°C, 3250 bars, to 280°C, 1600 bars. Lithium-rich pegmatite magmas from which spodumene or petalite crystallize early probably are emplaced at higher temperatures than their host rocks but below about 700°C (the upper stability limit for petalite and spodumene). The apparent inflection point in the Tanco cooling curve between points D and E in Figure 5E may correspond to attainment of thermal equilibrium with host rocks at P-T conditions that are below the greenschist-amphibolite metamorphic facies boundary and the aluminosilicate triple point (see Černý, 1982; London, 1984b; London and Morgan, 1985; Morgan and London, 1985). Thus, the portion of the Tanco cooling path from D to H (Fig. 5E) might reflect the cooling and uplift history of the Archean Superior province rocks that host the pegmatite. East from Tanco, pegmatites record higher-pressure lithium aluminosilicate assemblages, lesser fractionation, and deeper exposures of the plutonic sources of the pegmatites (Černý et al., 1981; Goad and Černý, 1981); the present erosional surface appears to reflect rotational uplift, with deeper rocks exposed to the east from Tanco. Similar evaluations of lithium aluminosilicate assemblages could aid in understanding regional P-T gradients and uplift histories of metamorphic terranes elsewhere.

Roles of Li, B, and tourmaline in pegmatite systems

The experimental results of Pichavant (1981, 1983), coupled with the observations of this study, indicate that the addition of boron to hydrous granitic melt produces an alkali tetraborate melt species; lithium tetraborate appears to be formed in preference to the sodium analogue. With the creation or addition of an alkali borate component, the solubility of H_2O (and incompatible trace elements) in silicate melt increases significantly (especially with increasing bulk alkalinity), with the possibility that at the P-T conditions of rare-element pegmatites, alkali borate contents may be sufficiently high that complete miscibility between silicate liquid and H_2O may exist; thus in principle, the transition from magmatic to hydrothermal conditions may be continuous. Whether or not these high borate contents are achieved depends on the stability of tourmaline, which is the only common sink for boron. The stable nucleation and growth of tourmaline apparently played a crucial role in the evolution of Tanco and probably many similar deposits.

Fluid-inclusion evidence from Tanco points to a significant change in fluid chemistry between 470 and 420°C and between 2900 and 2600 bars (interval between C and D, Fig. 5); the alkali borosilicate components appear to have been precipitated over this narrow P-T interval. The evolution of the fluid system at Tanco apparently required that (1) tourmaline did not crystallize throughout much of pegmatite crystallization, thus allowing concentration of the $Li_2B_4O_7$ component by fractionation and possibly by liquid immiscibility, and (2) significant amounts of tourmaline crystallized within or outside of the pegmatite system (i.e., in the wall rocks) between about 470 and 420°C and between 2900 and 2600 bars, thus depleting the Tanco fluid in the fluxing component $Li_2B_4O_7$, with the consequent deposition of alkali aluminosilicate and oxide ore components and exsolution of a relatively solute-poor aqueous fluid.

A number of factors may determine the stability of tourmaline. At Tanco, the boron contents of the inclusions in spodumene are far in excess of those needed to produce tourmaline in granitic systems (e.g., Pichavant, 1981, 1983), so that other parameters probably controlled the formation of tourmaline. The crystallization of tourmaline may be dependent in part on fluid acidity:

$$10\ \underset{\text{elbaite}}{NaLi_3Al_7(BO_3)_3Si_6O_{18}(OH)_4} + 6\ \underset{\text{quartz}}{SiO_2} + 6\ H_3BO_3 + 19\ H_2O$$
$$= 12\ \underset{\text{cookeite}}{LiAl_5Si_3O_{10}(OH)_8} + 10\ \underset{\text{albite}}{NaAlSi_3O_8} + 9\ Li_2B_4O_7.$$

The products of this reaction are present as daughter minerals within the inclusions hosted by spodumene. From the reaction above, it is apparent that the crystallization of tourmaline liberates an acidic aqueous fluid, and such a fluid may have been responsible for the subsequent late-stage conversion of feldspar to mica; an estimated 70% of the microcline-rich zones (4) and (6) at Tanco was replaced by mica + quartz (P. J. Vanstone, 1985, pers. comm.) during a stage of acid metasomatism that followed the crystallization of petalite and its subsequent replacement by spodumene + quartz.

One important control on tourmaline stability may be the coordination of boron (^{IV}B versus ^{III}B) in the pegmatitic melt; increases in $^{IV}B/^{III}B$ should inhibit the growth of tourmaline, in which boron is in trigonal coordination. Pichavant (1981) has suggested that $^{IV}B/^{III}B$ increases with increasing pressure; however, this does not satisfactorily explain the absence of tourmaline in that late stages of pegmatite crystallization, because most pegmatites (including Tanco) contain tourmaline that precipitated in the border zones, internal ore-bearing albitic aplites and cleavelandite complexes, and in the wall rocks. The $^{IV}B/^{III}B$ of anhydrous alkali borosilicate glasses increases with increasing alkalinity (i.e., with increasing alkali/aluminum and alkali/silica: Konijnendijk and Stevels, 1978; Bray, 1978). This change is consistent with Lewis acid-base principles: with increasing alkalinity, ^{IV}B oxyanions should be more effective than ^{III}B anions at shielding the positive charge on B^{3+}, and the anionic strength (basicity) of ^{IV}B oxyanions should be greater than ^{III}B units. In the following analysis, boron is assumed to dissolve in silicate melt as an alkali tetraborate species (e.g., $Na_2B_4O_7$), which contains two ^{III}B and two ^{IV}B oxyanions per formula unit (e.g., Bray, 1978; see also Burnham and Nekvasil, 1986); however, the speciation of boron (as well as the $^{III}B/^{IV}B$ ratio) varies significantly with the molar proportion of alkali/boron/silica (Dell et al., 1983). The speciation of boron in natural magmas can be expected to be complicated further by the presence of aluminum and other components (see Pichavant et al., 1984).

Additional controls on tourmaline stability may include temperature and the activities of ferromagnesian components. Foit and Rosenberg (1979) observed that the occupancy of the Y-site (the 9b site) in tourmaline may be in part temperature dependent. Tourmaline substitutions can be rationalized on the basis of a decrease in the mean polyhedral volume of the Y or 9b site with decreasing temperature; larger cations (Fe^{2+}) are incorporated at higher temperatures, and smaller cations (Al^{3+}) at lower temperatures. The activities of ferromagnesian components in highly fractionated pegmatites may not be high enough to stabilize schorl, and temperatures may generally be too high to crystallize Al-rich elbaites at early stages of consolidation. The apparent instability of Li-Al tourmalines is manifest at the Li-rich Harding pegmatite, New Mexico, which contains no tourmaline but produced extensive late-stage tourmalinization (to schorl) of mafic wall works (London, 1984c). Similarly, high concentrations of tourmaline (elbaites) are restricted to the late-stage pockets of miarolitic pegmatites (e.g., Foord, 1976; Taylor et al., 1979; London, 1986). These features suggest that in the *P-T* range in which these pegmatites form, the free energy of formation of schorl is significantly less than that of elbaite. As a result, (1) the crystallization of tourmaline (as schorl) requires an addition of ferromagnesian components to the pegmatite by fluid mixing within or at the margins of the body, or (2) in the absence of ferromagnesian components, the activity of the alkali borate component increases with decreasing *T* until elbaite becomes stable, or until boron is lost to the wall rocks (to form schorl) during the late stages of pegmatite consolidation.

An important and unresolved question is how the peralkaline borosilicate fluid was generated during crystallization of the Tanco magma. One requisite condition was that tourmaline did not crystallize throughout pegmatite consolidation, thus promoting high boron contents of residual fluids. The peralkalinity of the borosilicate fluid suggests that this liquid was in equilibrium with a peraluminous phase, but not tourmaline. Burnham and Nekvasil (1986) have proposed that boron interacts with haplogranitic melt by the formation of an alkali tetraborate species (Li or Na, but not K species). If, for the reasons cited above, tourmaline was not a stable phase, then the creation of lithium or sodium tetraborate melt species should have led to an expansion of the stability field and ultimate precipitation of primary muscovite. The pertinent reaction—

$$4\ \underset{\text{tourmaline}}{Na(\square Al_8)(BO_3)_3Si_6O_{18}(OH)_4} + 19\ \underset{\text{microcline}}{(K_{0.9}Na_{0.1})AlSi_3O_8} + 9\ \underset{V}{H_2O}$$
$$= 3\ Na_2B_4O_7 + 17\ \underset{\text{muscovite}}{KAl_3Si_3O_{10}(OH)_2} + 30\ \underset{\text{quartz}}{SiO_2},$$

in which sodium tetraborate is a melt component—apparently goes to the right throughout much of pegmatite crystallization. Upon subsequent crystallization of tourmaline, the excess alkali components of the borosilicate fluid may have promoted feldspar crystallization without micas (e.g., typical late-stage albitites or orthoclase-microcline) or may have been lost to wall rocks (a broad zone of intense alkali metasomatism of host rocks surrounds Tanco and most similar deposits).

In general, the crystallization of tourmaline at any stage of pegmatite consolidation should liberate large quantities of acidic aqueous fluid from silicate magma and will raise the solidus temperature of the remaining silicate liquid. Formation of tourmaline promotes further volatile loss and silicate crystallization if boron is partitioned into the exsolving aqueous fluid (boron $K_D = 3$: Pichavant, 1981); thus, stable growth of tourmaline may cause "boron quench" of pegmatitic magmas and may play a significant

role in controlling the timing and extent of H_2O exsolution and creation of a separate volatile phase. Crystallization of hydrous alkali borosilicate fluid to tourmaline + albite + quartz may produce pegmatitic pockets by the evolution of aqueous fluid, which expands against largely solidified pegmatite and ultimately may lead to pocket rupture (cf. Foord, 1976; London, 1986). At Tanco, volumetric expansion upon release of this aqueous fluid may have promoted fracturing of quartz that led to entrapment of successive generations of secondary aqueous inclusions.

Fluid inclusions in spodumene near the western tantalum ore body at Tanco contain the assemblage that has been described previously, plus a small, brown, isotropic daughter mineral with high relief (Fig. 2C). The phase is tentatively identified (by EDS) as microlite, which is abundant in the adjacent albite-mica ore unit. The apparent presence of microlite daughter crystals gives some measure of the solubility of rare metals in the hydrous alkali borosilicate fluid and suggests that rare-metal ores were precipitated from concentrated rather than dilute solutions. The borosilicate liquid represented by inclusions in Tanco spodumene appears to constitute the fluid from which the rare-metal albitites were deposited; thus the Ta- and Sn-rich albitites are primary in origin. Thomas and Spooner (1984) came to a similar conclusion based on field and petrographic analysis. Tourmaline-rich albitites commonly host rare-metal deposits in pegmatites throughout the world. It is probable that these deposits formed by a mechanism similar to that proposed for Tanco. From the preliminary experimental data in the system $LiAlSiO_4$-$NaAlSi_3O_8$-SiO_2-$Li_2B_4O_7$-H_2O, the addition of boron and creation of an alkali borate melt species apparently serve to promote extensive depolymerization of the silicate fluid, with concomitant enhancement of rare-metal solubilities by the creation of additional melt sites for incompatible low field-strength (e.g., Cs) and high field-strength (e.g., Ta) cations. Addition of B_2O_3 to anhydrous alkali aluminosilicate melts has been shown to significantly increase the solubilities of high charge-density cations (e.g., Bonniaud et al., 1978). At elevated fluid pressures, the combined effects of H_2O and B may further enhance the solubilities of incompatible lithophile elements. Whether B species are complexed with rare metals (other than Li and Na?) is not known, but the frequently observed spatial separation of tourmaline-rich zones and mineralized albite-mica units suggests that it is not. With regard to metal solubilities, the component $Li_2B_4O_7$ may behave like F and serve mainly to depolymerize melts, with consequent enhancement of H_2O and metal solubilities (e.g., Manning et al., 1980; Pichavant, 1981, 1983; Candella and Holland, 1983; Tingle and Fenn, 1984). The full role of boron will not be understood until its speciation in hydrous alkali borosilicate liquids has been resolved.

Conclusion

The results of the Tanco study indicate that existing models of crystallization in Li- and B-rich pegmatites and compositionally similar granites (e.g., Cornwall, England) may not adequately account for the properties and chemical evolution of fluids in these systems. The framework of the Jahns-Burnham model for pegmatite consolidation (Jahns and Burnham, 1969) entails crystallization from granitic silicate liquid and a coexisting, comparatively low-density, saline aqueous fluid with virtually no dissolved aluminosilicate components (e.g., Burnham, 1979). On the basis of fluid-inclusion data from Tanco, there is no indication that an exsolved aqueous fluid existed in the early stages of pegmatite consolidation; however, early separation of an aqueous phase would be expected in compositionally simple pegmatites, or in rare-element pegmatites in which early and continuous crystallization of tourmaline buffered boron contents at low values. This study presents evidence for dense, hydrous, alkali borosilicate fluids that are compositionally intermediate between granitic melt and hydrothermal aqueous fluid. A possible consequence of the high alkali borate content of such fluids at Tanco and elsewhere is immiscibility between silica- and alkali borosilicate–rich fluids that leads to crystallization of massive quartz bodies and adjacent rare-metal-rich albitites. In principle, the transition from magmatic to hydrothermal conditions may be continuous (i.e., supercritical) if sufficiently high concentrations of alkali borates are generated and retained in the fluid. The crystallization of tourmaline removes fluxing components and leads to precipitation of other alkali aluminosilicates and ore minerals, and to exsolution of a relatively low-density, solute-poor aqueous fluid. At Tanco, the borosilicate fluid and aqueous fluid derived from it possess comparatively low halide concentrations (salinities); high-salinity aqueous fluids were present only in the latest stages of subsolidus recrystallization. This and similar observations from other pegmatites (e.g., Foord, 1976; London, 1986) raise the question of the efficacy of H_2O in promoting chemical segregation in pegmatites if primary fluids do not contain appreciable halide salts, and especially if a separate aqueous phase does not exist. At Tanco, it appears that boron played an important role in the internal evolution of the pegmatite, including the concentration and deposition of rare-metal ore units. Possibly the most important role of alkali borate was in enhancement of H_2O solubility in silicate-rich fluids. Concomitant increases in alkali borate and H_2O can be expected to promote relatively rapid and efficient diffusion of components through a highly depolymerized silicate fluid medium with low viscosity, leading to chemical segregation and coarse-grained textures; these effects are confirmed by the exceedingly rapid crystal growth and low viscosities as observed in vapor-undersaturated runs in the system $LiAlSiO_4$-$NaAlSi_3O_8$-SiO_2-$Li_2B_4O_7$-H_2O. Crystallization of albite–tourmaline–quartz–Li-mica units may be regarded as the end stage of magmatic crystallization, and the consequent evolution of aqueous fluid marks the onset of subsolidus conditions. This late-stage aqueous fluid may be responsible for pseudomorphic metasomatism of early-formed minerals (e.g., London and Burt, 1982a, 1982c) and for alteration of pegmatite host rocks.

Although many simple and complex pegmatites contain tourmaline either within internal units or in tourmalinized

wall rocks, not all pegmatites display such obvious concentrations of boron. High activities of alkali borate probably are not the sole cause of chemical zonation and rare-element concentration in pegmatite systems; however, alkali borate apparently has a significant effect on phase equilibria and trace-element concentration in hydrous granitic melts, and these effects are consistent with many of the observed textural and paragenetic features of rare-element pegmatites.

Acknowledgments

Thanks especially to Edwin Roedder for comments and guidance throughout this study and to E. T. C. Spooner and H. S. Yoder, Jr. (Geophysical Laboratory, Washington, D.C.) for assistance in the initial stages of the project. M. J. Holdaway performed some of the hydrothermal runs for homogenization of spodumene inclusion contents. The manuscript has benefited from reviews by C. W. Burnham, R. C. Ewing, Edwin Roedder, and H. S. Yoder, Jr., and comments from numerous colleagues; the interpretations presented here, however, are my own and are not necessarily shared by the reviewers.

Funding was provided by grants from the University of Oklahoma Research Council, the University of Oklahoma Foundation, and the Oklahoma Mining and Mineral Resources Research Institute (R. H. Arndt, director) of the U.S. Bureau of Mines (Allotment Grant G-1154140).

References

Angus, S., Armstrong, B., de Reuk, K.M., Altunin, V.V., Gadetskii, O.G., Chapala, G.A., and Rowlinson, J.S. (1973) International tables of the fluid state: Carbon dioxide. Pergamon Press, New York.

Bazarov, L.S. (1975) Genesis of spodumene rare-metal pegmatites. In V.S. Sobolev, Ed. Mineralogy of endogenic formations from fluid inclusions in minerals (in Russian), 155–160. Western Siberian Publishing House, Novosibirsk (transl. abs. in Edwin Roedder, Ed., Fluid Inclusion Research, Proceedings of COFFI, 8, 19, 1975).

Bazarov, L.S., and Orlova, L.M. (1976) Character of changes of chemical composition of solution-melts in the process of crystallization of minerals in rare-metal pegmatites (in Russian). In Yu.A. Dolgov et al., Eds. Genetic studies in mineralogy, 106–115. Novosibirsk Institute of Geology and Geophysics, Siberian Branch, Akademii Nauk SSSR (transl. abs. in Edwin Roedder, Ed. Fluid inclusion research, Proceedings of COFFI, 10, 22, 1977.

Benard, F., Moutou, P., and Pichavant, Michel. (1985) Phase relations of tourmaline leucogranites and the significance of tourmaline in silicic magmas. Journal of Geology, 93, 271–291.

Beus, A.A. (1960) Geochemistry of beryllium and genetic types of beryllium deposits. Akademii Nauk SSSR, Moscow (transl. W.E. Freeman, San Francisco, 1967).

Bodnar, R.J. (1983) A method of calculating fluid inclusion volumes based on vapor bubble diameters and *P-V-T-X* properties of inclusion fluids. Economic Geology, 78, 535–542.

Bonniaud, R., Redon, A., and Sombret, C. (1978) Application of borate glasses and various boron-bearing glasses to the management of French radioactive wastes. In L.D. Pye, V.D. Frenchette, and N.J. Kreidl, Eds. Borate glasses: Structure, properties, applications. Materials Science Research, 12, 597–616. Plenum Press, New York.

Bowers, T.S., and Helgeson, H.C. (1983a) Calculation of the thermodynamic and geochemical consequences of nonideal mixing in the system H_2O-CO_2-NaCl on phase relations in geologic systems: Equation of state for H_2O-CO_2-NaCl fluids at high pressures and temperatures. Geochimica et Cosmochimica Acta, 47, 1247–1275.

——— (1983b) Calculation of the thermodynamic and geochemical consequences of nonideal mixing in the system H_2O-CO_2-NaCl on phase relations in geologic systems: Metamorphic equilibria at high pressures and temperatures. American Mineralogist, 68, 1059–1075.

Boyarskaya, R.V., Dolomanova, Ye.I., Nosik, L.P., and Fadyukov, Ye.M. (1977) Morphology and chemical compositions of inclusions of parent solutions in reticulate quartz from pegmatites of Volhyn, data of scanning electron microscopy and mass spectrometry (in Russian). In Ye.K. Lozarenko, Ed. Problems of regional and genetic mineralogy, 98, 1–8. "Naukova Dumka" Publishing House, Kiev (transl. abs. in Edwin Roedder, Ed. Fluid inclusion research, Proceedings of COFFI, 10, 34, 1977).

Bray, P.J. (1978) NMR studies of borates. In L.D. Pye, V.D. Frenchette, and N.J. Kreidl, Eds. Borate glasses: Structure, properties, applications. Materials Science Research, 12, 321–351. Plenum Press, New York.

Brookins, D.G., Chakoumakos, B.C., Cook, C.W., Ewing, R.C., Landis, G.P., and Register, M.E. (1979) The Harding pegmatite: Summary of recent research. New Mexico Geological Society Guidebook, 30th Field Conference, Santa Fe Country, 127–133.

Burnham, C.W. (1979) Magmas and hydrothermal fluids. In H.L. Barnes, Ed. Geochemistry of hydrothermal ore deposits, 2nd edition, 71–136. Wiley, New York.

Burnham, C.W., and Davis, N.F. (1971) The role of H_2O in silicate melts: I. *P-V-T* relations in the system $NaAlSi_3O_8$-H_2O to 10 kilobars and 1000°C. American Journal of Science, 270, 54–79.

Burnham, C.W., and Jahns, R.H. (1961) Experimental studies of pegmatite genesis: The composition of pegmatite fluids. Geological Society of America Special Paper 68, 143–144.

Burnham, C.W., and Nekvasil, Hanna. (1986) Equilibrium properties of granite pegmatite magmas. American Mineralogist, 71, 239–263.

Cameron, E.N., Rowe, R.B., and Weiss, P.L. (1953) Fluid inclusions in beryl and quartz from pegmatites in the Middletown district, Connecticut. American Mineralogist, 38, 218–262.

Candella, P.A., and Holland, H.D. (1983) The partitioning of copper and molybdenum between silicate melts and aqueous fluids. Geochimica et Cosmochimica Acta, 48, 373–380.

Černý, Petr. (1972a) The Tanco pegmatite at Bernic Lake, Manitoba. VIII. Secondary minerals from the spodumene-rich zones. Canadian Mineralogist, 11, 714–726.

——— (1972b) The Tanco pegmatite at Bernic Lake, Manitoba. VII. Eucryptite. Canadian Mineralogist, 11, 708–713.

——— (1975) Granitic pegmatites and their minerals: Examples of recent progress. Fortschritte der Mineralogie, Special Volume 52 (Papers and Proceedings of the 9th Meeting of the International Mineralogical Association, 1974, 225–250.

——— (1982) Petrogenesis of granitic pegmatites. In Petr Černý, Ed. Granitic pegmatites in science and industry, 405–461. Mineralogical Association of Canada Short Course Handbook 8.

Černý, Petr, and Ferguson, R.B. (1972) The Tanco pegmatite at Bernic Lake, Manitoba. IV. Petalite and spodumene relations. Canadian Mineralogist, 11, 660–678.

Černý, Petr, Trueman, D.L., Ziehlke, D.V., Goad, B.E., and Paul, B.J. (1981) The Cat Lake–Winnipeg River and Wekusko Lake pegmatite fields, Manitoba. Manitoba Department of Energy and Mines, Mineral Resources Division, Economic Geology Report ER80-1.

Charles, R.J., and Wagstaff, F.E. (1968) Metastable immiscibility in the B_2O_3-SiO_2 system. American Ceramics Society Journal, 51, 16–20.

Chorlton, L.B., and Martin, R.F. (1978) The effect of boron on the granite solidus. Canadian Mineralogist, 16, 239–244.

Collins, P.L.F. (1979) Gas hydrates in CO_2-bearing fluid inclusions and the use of freezing data for estimation of salinity. Economic Geology, 74, 1435–1444.

Cook, C.W. (1979) Fluid inclusions and petrogenesis of the Harding pegmatite, Taos County, New Mexico. M.S. thesis, University of New Mexico, Albuquerque.

Crawford, M.L. (1981) Phase equilibria in aqueous fluid inclusions. In L.S. Hollister and M.L. Crawford, Eds. Fluid inclusions—Applications to petrology, 75–100. Mineralogical Association of Canada Short Course Handbook 6.

Crouse, R.A., Černý, Petr, Trueman, D.L. and Burt, R.O. (1979) The Tanco pegmatite, southeastern Manitoba. Canadian Institute of Mining and Metallurgy Bulletin, 1979 (2), 1–10.

Dell, W.J., Bray, P.J., and Xiao, S.Z. (1983) ^{11}B NMR studies and structural modeling of Na_2O-B_2O_3-SiO_2 glasses of high soda content. Journal of Non-Crystalline Solids, 58, 1–16.

Foit, F.F., Jr., and Rosenberg, P.E. (1979) The structure of vanadium-bearing tourmaline and its implications regarding tourmaline solid solutions. American Mineralogist, 64, 788–798.

Foord, E.E. (1976) Mineralogy and petrogenesis of layered pegmatite-aplite dikes in the Mesa Grande district, San Diego County, California. Ph.D. thesis, Stanford University, Stanford, California.

Foord, E.E., Starkey, H.C., and Taggart, J.E., Jr. (1986) Mineralogy and paragenesis of "pocket" clays and associated minerals in complex granitic pegmatites, San Diego County, California. American Mineralogist, 71, 428–439.

Goad, B.E., and Černý, Petr. (1981) Peraluminous pegmatitic granites and their pegmatite aureoles in the Winnipeg River pegmatite district, southeastern Manitoba. Canadian Mineralogist, 19, 177–194.

Hervig, R.L., and Navrotsky, Alexandra. (1985) Thermochemistry of sodium borosilicate glasses. American Ceramics Society Journal, 68, 314–319.

Hollister, L.S. (1981) Information intrinsically available from fluid inclusions. In L.S. Hollister and M.L. Crawford, Eds. Fluid inclusions—Applications to petrology, 1–12. Mineralogical Association of Canada Short Course Handbook 6.

Jahns, R.H. (1982) Internal evolution of pegmatite bodies. In Petr Černý, Ed. Granitic pegmatites in science and industry, 293–327. Mineralogical Association of Canada Short Course Handbook 8.

Jahns, R.H., and Burnham, C.W. (1958) Experimental studies of pegmatite genesis: Melting and crystallization of granite and pegmatite. (abs.) Geological Society of America Bulletin, 69, 1592–1593.

——— (1969) Experimental studies of pegmatite genesis: I. A model for the derivation and crystallization of granitic pegmatites. Economic Geology, 64, 843–864.

Jahns, R.H., and Tuttle, O.F. (1963) Layered pegmatite-aplite intrusives. Mineralogical Society of America Special Paper, 1, 78–92.

Jolliff, B.L., Papike, J.J., Shearer, C.K., and Laul, J.C. (1986) Tourmaline as a recorder of pegmatite evolution: Bob Ingersoll pegmatite, Black Hills, South Dakota. American Mineralogist, 71, 472–500.

Kazamirova, T.K. (1976) Inclusions of solutions-melts in spodumene from rare-metal pegmatites (in Russian). Abstracts of the Fifth All-Union Conference on Thermobarogeochemistry, Akademii Nauk SSSR, Bashir Section, 115 (transl. in Edwin Roedder, Ed. Fluid Inclusion Research, Proceedings of COFFI, 10, 120, 1977).

Konijnendijk, W.L., and Stevels, J.M. (1978) Structure of borate and borosilicate glasses by Raman spectroscopy. In L.D. Pye, V.D. Frenchette, and N.J. Kreidl, Eds. Borate glasses: structure, properties, applications. Materials Science Research, 12, 259–279. Plenum Press, New York.

Koster van Groos, A.F., and Wyllie, P.J. (1966) Liquid immiscibility in the system Na_2O-Al_2O_3-SiO_2-CO_2 at pressures to 1 kilobar. American Journal of Science, 264, 234–255.

——— (1968) Melting relationships in the system $NaAlSi_3O_8$-NaF-H_2O to 4 kilobars. Journal of Geology, 76, 50–70.

Kovalenko, V.I., Antipin, V.S., Konusova, V.V., Smirnova, Ye. V., Petrov, L.L., Vladykin, N.V., Kuznetsova, A.I., Kostyukova, Ye.S., and Pisarskaya, V.A. (1973) Partition coefficients of fluorine, niobium, tantalum, lanthanum, ytterbium, tin, and tungsten in ongonite (in Russian). Doklady Akademii Nauk SSSR, 233, 951–953 (transl. Reports of the Academy of Sciences Earth Sciences Sections, 233, 203–205, 1973).

Kazlowski, A., and Karwowski, L. (1973) Hydrated salt melt as mineral forming medium of high-temperature associations from Alam Kuh (Iran) (in Russian). Abstracts of papers at Fourth Regional Conference on Thermobarogeochemistry of Mineral Forming Processes, Rostov University Press (transl. in Edwin Roedder, Ed. Fluid inclusion research, Proceedings of COFFI, 7, 113–114, 1974).

Krogh-Moe, Jans. (1962) The crystal structure of lithium diborate, $Li_2O \cdot 2B_2O_3$. Acta Crystallografia, 15, 190–193.

Lemmlein, G.G., Kliya, M.O., and Ostrkovskii, I.A. (1962) The conditions of formation of minerals in pegmatites according to data on primary inclusions in topaz (in Russian). Akademii Nauk SSSR Doklady, 142, 81–83 (transl. Soviet Physics—Reports, 7, 4–6, 1962).

Litovchenko, Ye.I. (1976) Genetic relations of minerals and inclusions of mineral-forming solutions as a reflection of the conditions of formation of pegmatites from western Priazov'ye (Ukranian Shield) (in Russian). (abs.) Problems of genetic information in mineralogy, proceedings of the All-Union Mineralogical Seminar, Stktyvkar, 108–109 (transl. in Edwin Roedder, Ed. Fluid inclusion research, Proceedings of COFFI, 10, 160, 1977).

London, David. (1981) Preliminary experimental results in the system $LiAlSiO_4$-SiO_2-H_2O. Carnegie Institution of Washington Year Book 80, 341–345.

——— (1982) Fluid-solid inclusions in spodumene from the Tanco pegmatite, Bernic Lake, Manitoba. Geological Society of American Abstracts with Programs, 14, 549.

——— (1983) The magmatic-hydrothermal transition in rare-metal pegmatites: Fluid inclusion evidence from the Tanco mine, Manitoba. (abs.) EOS (American Geophysical Union Transactions), 64, 549.

——— (1984a) Experimental phase equilibria in the system $LiAlSiO_4$-SiO_2-H_2O: A petrogenetic grid for lithium-rich pegmatites. American Mineralogist, 69, 995–1004.

——— (1984b) The role of lithium and boron in fluid evolution and ore deposition in rare-metal pegmatites. Geological Society of America Abstracts with Programs, 16, 578.

——— (1984c) Holmquistite, tourmaline, and wall-rock alteration around rare-metal pegmatites. (abs.) EOS (American Geophysical Union Transactions), 65, 1124.

——— (1985) Origin and significance of inclusions in quartz: A cautionary example from the Tanco pegmatite, Manitoba. Economic Geology, 80, 1988–1995.

——— (1986) Formation of tourmaline-rich gem pockets in miarolitic pegmatites. American Mineralogist, 71, 396–405.

London, David, and Burt, D.M. (1982a) Alteration of spodumene, montebrasite, and lithiophilite in pegmatites of the White Picacho district, Arizona. American Mineralogist, 67, 97–113.

——— (1982b) Lithium aluminosilicate occurrences in pegmatites and the lithium aluminosilicate phase diagram. American Mineralogist, 67, 483–493.

——— (1982c) Chemical models for lithium aluminosilicate stabilities in pegmatites and granites. American Mineralogist, 67, 494–509.

London, David, and Morgan, G.B., VI. (1985) Wall rock alteration around the Tanco rare-element pegmatite, Manitoba: Relations to pegmatite evolution. (abs.) (American Geophysical Union Transactions), 66, 1154.

London, David, Spooner, E.T.C., and Roedder, Edwin. (1982) Fluid-solid inclusions in spodumene from the Tanco pegmatite, Manitoba. Carnegie Institution of Washington Year Book 81, 334–339.

Luth, W.C., Jahns, R.H., and Tuttle, O.F. (1964) The granite system at pressures of 4 to 10 kilobars. Journal of Geophysical Research, 69, 759–773.

Makagon, V.M. (1973) Crystallization temperatures of lithium-bearing minerals in East Siberian rare-metal pegmatites (in Russian). Sibirskov Otdelenie Akademii Nauk SSSR, 133–138 (transl. abs. in Edwin Roedder, Ed. Fluid inclusion research, Proceedings of COFFI, 7, 133, 1974).

Manning, D.A.C. (1981) The effect of fluorine on liquidus phase relationships in the system Qz-Ab-Or with excess water at 1 kb. Contributions to Mineralogy and Petrology, 76, 206–215.

Manning, D.A.C., Hamilton, D.L., Henderson, C.M.B., and Dempsey, M.J. (1980) The probable occurrence of interstitial Al in hydrous, F-bearing and F-free aluminosilicate melts. Contributions to Mineralogy and Petrology, 75, 257–262.

Martin, J.S. (1983) An experimental study of the effects of lithium on the granite solidus. Ussher Society Journal, 5, 417–420.

Morey, G.W. (1951) Phase relations in the system Na_2O-B_2O_3-SiO_2. Society of Glass Technology Journal, 35, 270–283.

Morgan, G.B., VI, and London, David. (1985) Wall rock alteration around the Tanco rare-element pegmatite, Manitoba: Petrology of alteration halos. (abs.) EOS (American Geophysical Union Transactions), 66, 1153–1154.

Norton, J.J. (1983) Sequence of mineral assemblages in differentiated granitic pegmatites. Economic Geology, 78, 854–874.

Orlova, L.M., and Bazarov, L.S. (1975) Character of change of composition of volatiles during the process of formation of spodumene in pegmatites (in Russian). In V.S. Sobolev, Ed. Mineralogy of endogenic formations from inclusions in minerals. Western Siberian Publishing House, Novosibirsk, 33–36 (transl. abs. in Edwin Roedder, Ed. Fluid inclusion research, Proceedings of COFFI, 8, 137, 1975).

Pichavant, Michel. (1981) An experimental study of the effect of boron on a water saturated haplogranite at 1 kbar vapour pressure. Contributions to Mineralogy and Petrology, 76, 430–439.

——— (1983) Melt-fluid interaction deduced from studies of silicate-B_2O_3-H_2O systems at 1 kbar. Bulletin de Minéralogie, 106, 201–211.

Pichavant, Michel, and Ramboz, Claire. (1985) Liquidus phase relationships in the system Qz-Ab-Or-B_2O_3-H_2O at 1 kbar under H_2O undersaturated conditions and the effect of H_2O on phase relations in the haplogranite system. (abs.) Terra Cognita, 5, 230.

Pichavant, Michel, Schnapper, Denis, and Brown, W.L. (1984) Al = B substitution in alkali feldspars: Preliminary hydrothermal data in the system $NaAlSi_3O_8$-$NaBSi_3O_8$. Bulletin de Minéralogie, 107, 529–537.

Potter, R.W., II, Clynne, M.A., and Brown, D.L. (1978) Freezing point depression of aqueous sodium chloride solutions. Economic Geology, 73, 284–285.

Rockett, T.J., and Foster, W.R. (1965) Phase relations in the system boron oxide-silica. American Ceramics Society Journal, 48, 75–80.

——— (1966) The system silica-sodium tetraborate. American Ceramics Society Journal, 49, 30–33.

Roedder, Edwin. (1963) Studies of fluid inclusions II: Freezing data and their interpretation. Economic Geology, 58, 167–211.

——— (1968–1985) Fluid Inclusion Research—Proceedings of COFFI (an annual summary of World literature). Volume 1–5 (1968–1972) printed privately by the editor; volume 6 (1973) and onward printed by Ann Arbor Press, Ann Arbor, Michigan.

——— (1981) Natural occurrence and significance of fluids indicating high pressure and temperature. Physics and Chemistry of the Earth, 13, 9–39.

——— (1984) Fluid inclusions. Mineralogical Society of America Reviews in Mineralogy 12.

Roedder, Edwin, and Bodnar, R.J. (1980) Geologic pressure determinations from fluid inclusion studies. Annual Reviews of Earth and Planetary Sciences, 8, 263–301.

Rossovskii, L.N. (1981) Rare-element pegmatites with precious stones and conditions of their formation (Hindu Kush) (in Russian). Zapiski Vsesoyuznogo Mineralogicheskogo Obshchestva, 109, 301–311 (transl. International Geology Review, 23, 1312–1320, 1981).

Rossovskii, L.N., Makagon, V.M., and Kuz'mina, T.M. (1978) Characteristics of the formation of a kunzite deposit in Afghanistan (in Russian). Geologiya i Geofizika, 19, 102–109 (transl. Soviet Geology and Geophysics, 1, 82–87, 1979).

Stewart, D.B. (1978) Petrogenesis of lithium-rich pegmatites. American Mineralogist, 63, 970–980.

Taylor, B.E., and Friedrichsen, Hans. (1983) Light stable isotope systematics of granitic pegmatites from North America and Norway. Isotope Geoscience, 1, 127–167.

Taylor, B.E., Foord, E.E., and Friedrichsen, Hans. (1979) Stable isotope and fluid inclusion studies of gem-bearing granitic pegmatite-aplite dikes, San Diego County, California. Contributions to Mineralogy and Petrology, 68, 187–205.

Thomas, A.V., and Spooner, E.T.C. (1984) Petrological evidence for inward and upward non-replacive crystallization in the growth sequence lower wall zone, Ta(-Sn) bearing banded albitite, beryl fringe to quartz core, Tanco pegmatite, Manitoba. Geological Association of Canada Programs with Abstracts, 9, 111.

Tingle, T.N., and Fenn, P.M. (1984) Transport and concentration of molybdenum in granite systems: Effects of fluorine and sulfur. Geology, 12, 156–158.

Walker, R.J. (1985) The origin of the Tin Mountain pegmatite, Black Hills, South Dakota. Ph.D. dissertation, South Dakota School of Mines, Rapid City.

Weisbrod, Alain, and Poty, Bernard. (1975) Thermodynamics and geochemistry of the hydrothermal evolution of the Mayres pegmatite. Petrologie, 1, 1–16, 89–102.

Weiss, P.L. (1953) Fluid inclusions in minerals from zoned pegmatites in the Black Hills, South Dakota. American Mineralogist, 38, 671–697.

Wyllie, P.J., and Tuttle, O.F. (1961) Experimental investigation of silicate systems containing two volatile components. Part II. The effects of NH_3 and HF, in addition to H_2O, on the melting temperatures of albite and granite. American Journal of Science, 259, 128–143.

——— (1964) Experimental investigation of silicate systems containing two volatile components. Part III. The effects of SO_3, P_2O_5, HCl, and Li_2O, in addition to H_2O, on the melting temperatures of albite and granite. American Journal of Science, 262, 930–939.

Manuscript received January 7, 1985
Manuscript accepted October 14, 1985